DMD Fast Forward. Published on May 31, 2011 as doi:10.1124/dmd.110.036467

DMD#36467

METABOLISM OF [^{14}C]GSK977779 IN RATS AND ITS IMPLICATION WITH THE OBSERVED COVALENT BINDING

Catherine D Tsalta, Armina Madatian, Ernest M Schubert, Fangming Xia, William M Hardesty, Yanli Deng, Jennifer L Seymour and Peter D Gorycki

Preclinical Drug Metabolism and Pharmacokinetics, GlaxoSmithKline, King of Prussia, Pennsylvania

DMD Fast Forward. Published on May 31, 2011 as DOI: 10.1124/dmd.110.036467
This article has not been copyedited and formatted. The final version may differ from this version.

Running Title: Metabolism of [^{14}C]GSK977779 in Rats Leading to Covalent Binding

Corresponding Author: Catherine Tsalta, Drug Metabolism and Pharmacokinetics, GlaxoSmithKline, 709 Swedeland Rd., King of Prussia, PA 19406, USA

Tel: 610-270-5246

Fax: 610-270-5041

E-mail: Catherine.2.Tsalta@gsk.com

No. of Text Pages= 34

No. of tables = 11

No. of figures = 12

No. of references = 29

No. of words in:

Abstract = 166

Introduction = 314

Discussion = 1697

ABBREVIATIONS: SEC, size-exclusion chromatography; SDS, sodium dodecyl sulphate; HPLC, high-performance liquid chromatography; NA, Nicotinic acid, Niacin; NEFA, non-esterified fatty acids; ADME, absorption, disposition, metabolism and elimination; NADP and NADPH, nicotinamide adenine dinucleotide phosphate and its reduced form; PAGE, polyacrylamide gel electrophoresis; LC-MS/MS, liquid chromatography/tandem mass spectrometry; LC-MRM, liquid chromatography multiple reaction monitoring mass spectrometry; BDC, bile duct-cannulated; HPMC, hydroxypropyl methycellulose; LSC, liquid scintillation counting; TCA, trichloroacetic

acid; LLQ, lower limit of quantitation; CYP, cytochrome P_{450} enzymes; MALDI MS, matrix-assisted laser desorption/ionization mass spectrometry; Da, Dalton.

DMD Fast Forward. Published on May 31, 2011 as DOI: 10.1124/dmd.110.036467
This article has not been copyedited and formatted. The final version may differ from this version.

Abstract: GSK977779 is a potent HM74a agonist evaluated for the treatment of dyslipidemia. The disposition and metabolism of [^{14}C]GSK977779 (67.6 µmol/kg, p.o.) was studied in male and female rats. The compound was well absorbed with its primary route of elimination being in the feces. Based on metabolite profiling of plasma extracts, urine and bile samples, it was demonstrated that GSK977779 was extensively metabolized in the rat by N-dealkylation, mono- and di-oxygenation, reductive and oxidative cleavage of the 1, 2, 4-oxadiazole ring and conjugative pathways. Following plasma extraction high amounts of non-extractable radioactivity were observed which were more pronounced in female rats. Size-exclusion chromatography (SEC) and sodium dodecyl sulphate (SDS) gel electrophoresis indicated that the majority of the non-extractable radioactivity was covalently bound to plasma proteins. Solubilization of the plasma protein pellet followed by high-performance liquid chromatography (HPLC) and mass spectrometry (MS) suggested that a carboxylic acid metabolite derived from oxadiazole ring cleavage may be responsible for the observed covalent binding of the radioactivity to rat plasma proteins.

DMD Fast Forward. Published on May 31, 2011 as DOI: 10.1124/dmd.110.036467
This article has not been copyedited and formatted. The final version may differ from this version.

Introduction: GSK977779 is a potent and selective agonist of the HM74a receptor which was identified as a development candidate for the treatment of dyslipidemia. Nicotinic acid (NA) displays high affinity binding to HM74a, a seven transmembrane domain G-protein-coupled receptor which has been demonstrated to be responsible for the antilipolytic response to Niacin (Karpe and Frayn, 2004; Tunaru et al., 2003; Wise et al., 2003). Stimulation of the receptor by NA or synthetic agonists, such as acipimox or acifran, results in inhibition of adipocyte hormone-sensitive lipase activity and an acute decline in the concentration of non-esterified fatty acids (NEFA) in serum (Grundy et al., 1981; Fuccella et al., 1980). HM74a agonists decrease the plasma levels of triglycerides and low density lipoprotein cholesterol and increase the plasma levels of high density lipoprotein cholesterol. Based on head to head comparison in nonclinical models GSK977779 had the potential to be pharmacologically of similar or greater activity than Niacin and to provide a better tolerability profile in humans with respect to flushing.

As part of the nonclinical development program [^{14}C]GSK977779 (Figure 1) was administered orally to rats to determine the routes of elimination of the compound and the biotransformation pathways with emphasis on the identification and quantification of the circulating metabolites. In addition these studies assessed the extractability of the circulating radioactivity in order to investigate the potential for covalent binding of GSK977779 related material to plasma proteins. In this manuscript we describe the main pathways of biotransformation of GSK977779 in the rat and the evaluation of the covalent binding of GSK977779 to rat plasma proteins. The structural elucidation of the metabolites revealed several possibilities for formation of reactive intermediates leading to covalent binding which are discussed in this paper. The experimental methods used

for the evaluation of covalent binding which consisted of solvent extraction, size exclusion chromatography and sodium dodecyl sulphate polyacrylamide gel electrophoresis (SDS PAGE) are also described.

Materials and Methods

Chemicals. [^{14}C]GSK977779D (specific activity 6.52 μCi/mg, radiochemical purity 99.5%) and non-radiolabeled GSK977779 (chemical purity 99.4%) were synthesized and purified by Chemical Development, GlaxoSmithKline Pharmaceuticals (Stevenage, UK). The protein standards (Bio-Rad 161-0324) used for the SDS PAGE experiments were purchased from Bio-Rad Co. (Hercules, CA) and contained the following proteins (molecular weight): myosin (200,000) β-galactosidase (116,250), bovine serum albumin (BSA; 66,000) ovalbumin (45,000), carbonic anhydrase (31,000), soybean trypsin inhibitor (21,500) lysozyme (14,400) and aprotinin (6,500). In addition Laemmli buffer (62.5 mM Tris-HCl, pH 6.8, 2% SDS, 25% glycerol, 0.01% Bromophenol Blue), Tris/glycine/SDS (25 mM/192 mM/0.1%, respectively, pH 8.3) and 7.5% precast polyacrylamde minigels, 10 well, 8.6 X 6.8 cm were purchased from Bio-Rad for the SDS PAGE experiments. Pooled male or female human liver microsomes and rat liver microsomes were obtained from XenoTech LLC (Lenexa, KS). All other chemicals and reagents used were of general laboratory grade or better, and were purchased from standard commercial sources. Scintillation cocktails Ultima Gold and Ultima Flo M were obtained from PerkinElmer Life and Analytical Sciences (Boston, MA).

Dosing of Animals and Collection of Samples. All the animal studies were conducted after approval of protocols by the Institutional Animal Care and Use Committee in approved facilities.

Fifteen intact male and fifteen intact female Sprague Dawley rats and three bile duct-cannulated (BDC) male rats (Hilltop Lab Animals, Inc; Scottdale, PA) weighing

250-350 g each received a single oral administration of [^{14}C]GSK977779 at a target dose of 30 mg/kg (67.6 µmol/kg) as a suspension in 0.5% (w/v) aqueous hydroxypropyl methylcellulose (HPMC) at 3 mg/ml. Urine and feces were collected from three intact male and three intact female rats pre-dose and at various intervals through 168 h post-dose. Urine, bile and feces were collected from the three BDC rats pre-dose and post-dose at various intervals through 96 h post-dose. Blood was also collected from three intact animals/sex/time point at 2 h, 4 h, 8 h and 24 h post-dose as terminal bleeds. After a portion of blood had been removed for radioanalysis, the remaining blood was centrifuged to harvest the plasma. Animal cages were rinsed with deionized water following each daily excreta collection. After the last excreta samples were collected, the cages were washed with an ethanol:1% trisodium phosphate solution (1:1; v/v) and wiped with gauze pads. The residual carcasses were retained for bioanalysis. Blood was collected *via* exsanguination (under isofluorane anesthesia) from selected animals at euthanasia. All post-dose samples (bile, urine, feces, blood, plasma, cage rinse, cage wash, residual carcass, and extracts of the bile cannulas, jackets and cage wipes) were analyzed for total radioactivity.

Additional rats were dosed with [^{14}C]GSK977779 to generate plasma samples for SDS PAGE experiments. Six male and six female rats obtained from Charles River Laboratories (Wilmington, MA) and weighing 250-350 g were administered a single oral dose of either 3 mg/kg or 30 mg/kg of [^{14}C]GSK977779 (three animals/sex/dose group) as a suspension in 0.5% (w/v) aqueous HPMC at 0.3 mg/ml and 3 mg/ml, respectively. Blood was collected *via* exsanguination (under isofluorane anesthesia) from each animal at 2 h, 8 h or 24 h post-dose (one animal/sex/time point). After a portion of blood had

been removed for radioanalysis, the remaining blood was centrifuged to harvest plasma. An additional two female rats were subsequently dosed with 30 mg/kg of non-radiolabelled GSK977779 as a suspension in 0.5% (w/v) aqueous HPMC and blood was collected from these animals *via* exsanguination at 24 h post dose. The purpose of this experiment was to obtain plasma, subject it to an exhaustive extraction procedure which involved the precipitation of plasma protein, and analyze the plasma protein for the identity of the any GSK977779-related covalently bound moiety.

Determination of Radioactivity in Plasma, Urine, Bile, Liver and Feces.

Plasma, bile and urine samples were assayed for radioactivity by liquid scintillation counting (LSC) using Packard TriCarb 3100TR (PerkinElmer Life and Analytical Sciences Inc, Boston, MA) with counting efficiency determined by an external standard ratio procedure. Samples were counted for a preset time of 5 minutes. Where appropriate, samples were dispensed directly into Ultima Gold scintillation cocktail (10 ml). Liver and feces samples were mixed with water at an approximate weight ratio of 1:3. The samples were homogenized using a Polytron 10/35 probe-type homogenizer (Brinkmann Instruments Inc., Westbury, NY) and aliquots weighing 0.2 g each were combusted and analyzed for radioactivity. Combustion was performed with a Packard Oxidizer 307 utilizing Carbosorb E (8 ml) as the carbon dioxide absorber and Permaflour E+ (12 ml) as the scintillation cocktail. An aliquot of Combustaid (200 μL) was added to each sample prior to combustion. Aliquots of ^{14}C SPEC CHEC standard (PerKinElmer Life and Analytical Sciences) were combusted throughout the batch to determine oxidizer combustion efficiencies. To convert the radioactivity of sample (dpm/g) to concentration

DMD Fast Forward. Published on May 31, 2011 as DOI: 10.1124/dmd.110.036467
This article has not been copyedited and formatted. The final version may differ from this version.

units (µg eq GSK977779/gram of sample) a conversion factor of 14.49 dpm/ng was used based on the specific activity of the radiolabel.

Plasma and Liver Sample Preparation for Extractability Determination and Metabolite Profiling. Plasma and liver homogenate samples from individual animals were pooled across each time point using equal volumes (for plasma) or equal weights (for liver) to produce a single representative sample per time point (2, 4, 8 and 24 hours). Aliquots of the pooled rat plasma samples were counted by LSC prior to solvent extraction. Separate aliquots of plasma samples were extracted two times with four volumes of acetonitrile followed by centrifugation. The supernatants from the two extractions were combined and the total extracted radioactivity was determined by LSC. The combined supernatants were evaporated to dryness under nitrogen, reconstituted in 1:1 (v/v) methanol:25 mM ammonium formate pH 3.5 and analyzed for metabolite profiling by radio-HPLC.

Selected plasma samples which exhibited low extractability in acetonitrile (less than 90% recovery) were extracted exhaustively with 10% (w/v) trichloroacetic acid (TCA) followed by three times extraction with 4:1 (v/v) methanol:diethyl ether. Triplicate aliquots of the TCA extracts and the methanol/ether extracts were radioassayed to determine the percent recovery of radioactivity in these extracts. The amount of radioactivity recovered from the acetonitrile, TCA and methanol/ether extractions was reported as total extractable and was expressed as percentage of total sample radioactivity. The same plasma exhaustive extraction procedure (acetonitrile, followed by TCA and methanol: diethyl ether) was followed for the 24 h plasma generated from two rats dosed with non-radiolabelled GSK977779. The supernatants from this

DMD Fast Forward. Published on May 31, 2011 as DOI: 10.1124/dmd.110.036467
This article has not been copyedited and formatted. The final version may differ from this version.

extraction were not used for any further experimentation. Only the plasma protein pellet was analyzed further.

Aliquots of pooled liver homogenate samples were analyzed for radioactivity content before extraction. Separate aliquots (1 g) were then treated with approximately 4 volumes of methanol:water (1:3, v/v), vortex mixed, sonicated for at least 5 minutes and rotary mixed for at least 55 minutes. The samples were then centrifuged at approximately 3,100g_{av} using a Beckman AccuSpin FR centrifuge (Beckman Instruments Inc., Fullerton, CA) at ambient temperature for 5 minutes. The residue was extracted one additional time with the same solvent and the supernatant was combined with the original extract. The combined extracts were mixed, the total volume determined and triplicate aliquots (approximately 0.2 ml) were removed to determine total extracted radioactivity by LSC.

[^{14}C]GSK977779 dosing solution had been added to control rat plasma on the day of dosing. This sample was stored frozen under the same conditions as the other samples until the time of analysis. An aliquot of this spiked control sample was analyzed for total radioactivity by LSC. A separate aliquot was extracted by acetonitrile and the extract was analyzed by LSC to determine the recovery of radioactivity in the acetonitrile extract.

Solubilization and Analysis of Plasma Protein Pellet. Following extraction the residual plasma protein pellets were incubated with 1M NaOH (3 ml) at 50°C overnight for solubilization. Triplicate aliquots of the mixtures were removed, neutralized by the addition of an appropriate volume of glacial acetic acid, mixed with 10 ml of scintillation cocktail, and kept at room temperature for about 2 hours. Samples were then

radioassayed by LSC to determine the amount of non-extractable radioactivity in the pellets. Fifty microliter aliquots of the neutralized mixtures resulting from the solubilization of the 24 h female and male plasma pellets were injected onto HPLC for radioprofiling. A 24 h rat plasma pellet generated with non-radiolabelled GSK977779 compound was also incubated with 1M NaOH (3 ml) at 50°C overnight and subsequently neutralized by an appropriate volume of glacial acetic acid. An aliquot of 50 µl of the neutralized mixture was analyzed by HPLC-MS to determine the identity of the released GSK977779 related moiety(ies).

One hundred microliters of unlabelled GSK977779 (1 mM) in 100% acetonitrile was mixed with 900 µl of 1M NaOH and incubated overnight at 50°C. The solution was neutralized by the addition of an appropriate volume of glacial acetic acid. An aliquot of this solution was analyzed by LC-MS/MS to check the stability of GSK977779 under these conditions.

Urine and Bile Sample Preparation. A portion of the urine and bile samples were pooled by total weight ratio for each animal to obtain a representative sample accounting for the majority of the excreted radioactivity. Aliquots of urine and bile samples were analyzed by LSC for radioactivity determination. Separate aliquots were centrifuged and the supernatants analyzed by LC-MS/MS for quantification and identification of metabolites.

Microsomal Binding Assay. [^{14}C]GSK977779 (10 µM) was incubated with male and female pooled human or rat liver microsomes (0.5 mg total protein) and 0.1 ml of either NADPH generating system or 2% sodium bicarbonate solution in triplicate in a final volume of 0.5 ml of 0.1 M potassium phosphate buffer, pH 7.4 for 0, 30 and 60

DMD Fast Forward. Published on May 31, 2011 as DOI: 10.1124/dmd.110.036467
This article has not been copyedited and formatted. The final version may differ from this version.

minutes. The NADPH generating system was freshly prepared in 2% sodium carbonate solution and contained NADP, glucose-6-phosphate and glucose-6-phosphate dehydrogenase at concentrations of 1.7 mg/ml, 7.8 mg/ml and 6 units/ml, respectively. Incubations were also conducted in an identical manner with [^{14}C]acetaminophen (10 μM) for 0 and 60 minutes as a positive control. After termination of the incubations the reaction mixtures were filtered and the filters were washed five times with 4 ml methanol:water (90:10, v/v). The filters were then transferred to glass scintillation vials and analyzed for the retained radioactivity by LSC.

Glutathione Trapping Assay. Two hundred microliters of 2.5 mg/ml human liver S9 fractions, human liver microsomes or rat liver microsomes, 100 μl of 50 mM glutathione (GSH) in buffer and 100 μl of 0.5 mM GSK977779 or of the positive control 3-methylindole were incubated in 96-deepwell tubes at 37°C in a water bath. After 3 minutes pre-incubation, the reaction was initiated by adding an NADPH generating system (100 μl solution consisting of 2.22 mM NADP, 27.65 mM glucose-6-phosphate and 6.0 units/ml glucose-6-phosphate dehydrogenase together with 15 mM $MgCl_2$ in 0.1 M phosphate buffer). The final concentrations of the liver in vitro systems, GSK977779 and glutathione in the incubation mixture were 1 mg/ml, 100 μM and 10 mM, respectively. The enzymatic reactions were terminated after 90 minutes by the addition of 100 μl of acetonitrile containing 6% of acetic acid. In parallel, control incubations without the NADPH-generating system, GSH, liver protein matrix or GSK977779 were conducted. After protein precipitation the samples were centrifuged and 10 μl of the resulting supernatants were analyzed by UPLC-MS using an Acquity UPLC BEH C18 column (50 X 2 mm, 1.7 μM) and a Sciex API-5000 triple quadrupole

mass spectrometer with neutral loss scanning of 129 corresponding to the loss of pyroglutamic acid.

Size Exclusion Chromatography. Size exclusion chromatography was performed using Agilent 1100 systems similar to those used for radio-HPLC analysis described in the following section. Aliquots of pooled plasma samples were denatured with two volumes of 6M guanidine hydrochloride (Lot number 15914DE, Sigma Aldrich Inc, Spruce St. Louis, Mo) by vortex mixing for 30 seconds at room temperature. The denatured plasma samples (5-99 µl) were injected onto a BioSep-SEC-S3000 column, 300 X 7.8 mm, 5 µm, pore size 290Å (Phenomenex, Torrance, CA). In addition to the plasma samples, 50 µl of a standard solution containing 0.9 mg/ml albumin (high molecular weight standard) and 0.05 mg/ml GSK977779 (low molecular weight standard) was denatured by mixing with 100 µl 6M guanidine HCl and the mixture was injected onto the BioSep-SEC-S3000 column. HPLC analysis was carried out using an isocratic gradient of 6M guanidine HCl in water at a flow rate of 0.5 ml/min with a run time of 50 min. For the plasma samples fraction collection was done at 0.104 ml per fraction into four 96-well scintillation Luma™ microtitre plates. The solvent in the plates was evaporated to dryness at approximately 40˚C in an oven. The dried plates were then heat sealed using Top Seal S film (PerkinElmer) and analyzed using a Packard TopCount Scintillation Counter. The resulting TopCount data was imported into Laura software (LabLogic, Tampa, FL) using its LSC import function to construct radiochromatograms. The area under each peak was integrated and expressed as a percentage of the total counts detected. For the albumin and GSK977779 standards chromatographic run UV detection at 280 nm was used.

DMD Fast Forward. Published on May 31, 2011 as DOI: 10.1124/dmd.110.036467
This article has not been copyedited and formatted. The final version may differ from this version.

SDS Gel Electrophoresis. Plasma samples collected from individual rats administered either 3 or 30 mg/kg [^{14}C]GSK977779 were analyzed by SDS PAGE. Equal volumes of plasma collected at 2 and 24 h post-dose (~ 10 µl) and Laemmli buffer (Bio-Rad Co, Hercules, CA) were mixed and the mixture was heated to 95˚C for 3-5 min in a stirred water bath. After cooling to room temperature an aliquot of 1.5 µl of the plasma/buffer mixture was loaded per lane on 7.5% precast PAGE minigels (Bio-Rad Co). Three replicate lanes were created per sample. In addition, a mixture of protein molecular weight standards treated in the same manner as the plasma samples was applied on each gel along with the samples. Electrophoresis was performed in a Mini-Protean 3 cell apparatus (Bio-Rad Co) at 200 V, for about 35 min using Tris/glycine/SDS (Bio-Rad, Co) as the running buffer. The starting current was 50 mA and the ending current was 30 mA. Gels were fixed, stained with Coomassie Blue, destained and washed. Gel lanes were cut into five sections based on molecular weight: stacking gel, >120 kDa, 80-120 kDa, 20-80 kDa and <20 kDa. Gel sections and sample loads were combusted and analyzed by LSC. The radioactivity in each gel section was compared to the amount of radioactivity loaded onto each lane of the gel. The total percent of radioactivity retained in each lane was calculated by adding the recoveries of individual gel sections.

Radio–HPLC Metabolite Profiling. Radio-HPLC chromatograms were generated on Agilent 1100 systems (Agilent Technologies, Inc., Palo Alto, CA) equipped with a Diode Array UV Detector and connected to a β-RAM Model 2B radiometric detector (LabLogic, Tampa, FL) with a 500 µl homogeneous liquid scintillant flow cell and a built in liquid scintillant pump. A Synergi Fusion analytical column (4.6 X 250

DMD Fast Forward. Published on May 31, 2011 as DOI: 10.1124/dmd.110.036467
This article has not been copyedited and formatted. The final version may differ from this version.

mm, 4μm particle size, Phenomenex) connected with a guard column (Fusion RP, Phenomenex) was used for metabolite separation. Samples were eluted at a rate of 1 ml/min using a gradient which was comprised of 25 mM ammonium formate pH 3.5 (solvent A), and acetonitrile (solvent B). The gradient was as follows: Solvent B was held at 12% for the first 5 min and then increased linearly to 27% (5-20 min); it was then held at 27% B from 20 to 35 min, increased linearly to 57% (35-50 min), and then from 50 to 51 min ramped to 95% B and held for 7 min. At 58-59 min the gradient was returned to the initial condition (12% B) for a 9 min isocratic column re-equilibration. Urine and bile samples were analyzed with on-line radio-detection, during which the eluent was mixed with Ultima Flo M scintillant at a ratio of 1:3 by volume. Radioactivity data was collected at the rate of 1 point/second to plot the radioactive peaks. The percentage of radioactivity in each peak of the metabolic profile was calculated using Laura software (Version 3.3.10, LabLogic Inc., Tampa, FL) and expressed as the percentage of the administered dose recovered in urine and bile corrected for the centrifugation recovery. For plasma extracts that contained insufficient amounts of radioactivity for on-line radiometric detection, the HPLC eluent was collected into 96-well solid scintillant LUMA™ microtitre plates (PerkinElmer Life and Analytical Sciences, Inc., Boston, MA) using a Gilson 222XL liquid handler (Gilson, Inc., Middleton, WI) at 0.150 min/well. The solvent in the microtitre plates was evaporated to dryness at 40°C in an oven (Model 1320, VWR Scientific Products, Inc., Plainfield, NJ). The dried plates were then heat-sealed using Top-Seal S film (PerkinElmer) and analyzed using a PerkinElmer TopCount NXT scintillation counter. Each well was counted for 5 min without background subtraction. The resulting TopCount data was imported into the

Laura software (LabLogic, Tampa, FL) using its "LSC Import" function and processed by Microsoft Excel 2002 to reconstruct radio-HPLC chromatograms. Each radioactive peak was calculated as a percentage of the total counts detected. The total radioactivity contained in the acetonitrile extracts was also expressed as µg equivalents of GSK977779 per gram of plasma. The lower limit of quantification (LLQ) was defined as three times the background area integrated in each chromatogram.

Mass Spectrometric Analysis. Metabolite characterization was conducted by one or more of the following: LC-MS^n, LC-MRM, and LC-MS accurate mass analysis. The LC conditions were similar to those utilized for metabolite profiling as described above. HPLC eluent was split at 1:10 ratio between a mass spectrometer and a radiometric flow detector (Packard 515TR, Perkin Elmer, Waltham, MA). Nominal mass measurements and MS/MS experiments were performed on a Thermo Fisher LTQ mass spectrometer equipped with an ESI source (Thermo Fisher, San Jose, CA). Accurate mass measurements, defined as <5 ppm or <2mDa from the theoretical mass, were performed on a Waters QToF II equipped with an ESI source (Waters Corporation, Milford, MA). All instruments utilized a CTC PAL autosampler (LEAP Technologies, Carrboro, NC) for sample introduction. Data were acquired and processed using Xcalibur software (version 1.3, Thermo Fisher, San Jose, CA) or Masslynx software (version 3.5, Waters Corporation, Milford, MA).

Isolation of Metabolites and NMR Analysis. To confirm their structural assignments, metabolites M9, M11, M12, M14 and M5 were isolated from a rat bile sample which was generated through perfusion of a rat liver (procedure not described in this paper) and further analyzed by LC-MS/MS and NMR as described below.

DMD Fast Forward. Published on May 31, 2011 as DOI: 10.1124/dmd.110.036467
This article has not been copyedited and formatted. The final version may differ from this version.

An aliquot of the rat bile sample was injected onto an Agilent 1100 system equipped with Phenomenex Synergi Polar RP-80, 250 X 10 mm column connected with a Phenomenex Polar RP, 10 X 10 mm guard column. Metabolites were eluted using a gradient at a flow rate of 4.7 ml/min with solvents A (25 mM ammonium formate pH 3.5) and B (methanol). The following three step gradient was used: 30% solvent B (0-10 min), 30% to 80% B (10-110 min) with further increase to 95% B (110-121 min). After elution of GSK977779 and its metabolites, the gradient was switched back to 30% B and the column was thoroughly washed before the next injection. The column eluate containing each of the major radioactive peaks was collected into separate vials. The presence of each metabolite was confirmed by removing an aliquot of the fraction containing the metabolite of interest and analyzing by HPLC-MS. The LC-MS conditions were similar to those described in the above section using positive ionization in full scan mode.

The isolated M9, M11, M12, M14 and M5 samples were further analyzed by nuclear magnetic resonance (NMR) spectroscopy for definitive structural assignment. All spectra were obtained on a Bruker Avance DRX 700MHz NMR spectrometer (Bruker Biospin Corp., Billerica, MA) equipped with a 5mm TCI cryoprobe maintained at 298 K. Samples were dissolved in a mixture of acetonitrile-d_3 and D_2O (1:1, v/v). ^{1}H and ^{13}C NMR chemical shifts were referenced to the residual solvent signals of acetonitrile (δ_H 1.93 and δ_C 1.3 ppm), as appropriate. All NMR experiments conducted utilized pulse sequences coded in the standard Bruker software (TopSpin 2.0.4).

DMD Fast Forward. Published on May 31, 2011 as DOI: 10.1124/dmd.110.036467
This article has not been copyedited and formatted. The final version may differ from this version.

Results

Excretion Studies. The mean recoveries of [^{14}C]GSK977779 following single oral administration to rats at a dose of 30 mg/kg (195.6 µCi/kg) are shown in Table 1. The majority of radioactivity was excreted in the feces within 48 hours post-dose. The fraction of dose excreted by this route was higher in males (73.3%) than in females (58.3%). Conversely, urinary elimination in males (19.0%) was less than that observed in females (33.0%). In BDC animals, 52.1% of the dose was eliminated in the bile while additional 19.1% of the dose was eliminated in the urine. Based on the high percentage of radioactivity recovered in bile and urine of BDC animals (total of 71.2% of dose), it was concluded that [^{14}C]GSK977779 was well absorbed in the rat.

Plasma and Liver Extractability. The concentration of drug related material in the rat plasma and liver samples expressed as µg GSK977779 equivalents per gram of sample (µg/g) is presented in Table 2 and Table 3 respectively. The recoveries of radioactivity from pooled plasma samples as well as the amount of radioactivity remaining in the plasma pellet following solvent extraction are also shown in Table 2. In male rat plasma the extractable radioactivity decreased from approximately 87% at 2 h post-dose to 56.5% at 24 h. In female rat plasma the extractable radioactivity was 67% at 2 h and decreased to 6.3% at 24 h post-dose. At all time points the extractable radioactivity was significantly lower in females than in males. The amount of non-extractable radioactivity reached 81.9% of the total plasma radioactivity in females at 24 h post dose. Based on a concentration of 67 mg protein per gram of rat plasma (Davies and Morris, 1993) the non-extractable radioactivity in the female plasma sample at 24 h corresponded to 1182 pmol of GSK977779 equivalents per mg of plasma protein. In

DMD Fast Forward. Published on May 31, 2011 as DOI: 10.1124/dmd.110.036467
This article has not been copyedited and formatted. The final version may differ from this version.

male and female liver samples the amount of extractable radioactivity ranged from 85.1% to 98.1%. The lowest extractability was found with the 24 hour female liver sample. Based on a concentration of 162 mg protein per gram of rat liver (Saadane et al., 1996) the non-extractable radioactivity in the female 24 h liver sample corresponded to 18.4 pmol of GSK977779 equivalents per mg of liver protein.

Microsomal Binding Assay. The NADPH-dependent binding of radioactivity by human or rat male and female liver microsomes was calculated by subtracting the amount of filter retained radioactivity in the absence of NADPH from the filter retained radioactivity in the presence of NADPH. The results are shown in Table 4. Following 60 minutes of incubation the NADPH-dependent binding of [^{14}C]GSK977779 related radioactivity in male and female rat liver microsomes was 177 pmol/mg protein and 295 pmol/mg protein, respectively while for [^{14}C]acetaminophen it was 75.8 pmol/mg and 22.5 pmol/mg, respectively. In male and female human liver microsomes the NADPH-dependent binding of [^{14}C]GSK977779 related radioactivity was 136 pmol/mg and 132 pmol/mg protein, respectively while for [^{14}C]acetaminophen it was 104 pmol/mg and 158 pmol/mg, respectively.

Glutathione Trapping Assay. There was no GSH adduct of GSK977779 detected in this experiment. The performance of the positive control for GSH adduct formation (3-methylindole) was consistent with historical data and the literature (Yan et al., 2007).

Size Exclusion Chromatography. Figure 2 shows the UV (280 nm) chromatogram of the albumin and GSK977779 standards following mixing with 6M guanidine and size-exclusion chromatography. Figure 3 shows a representative size-

DMD Fast Forward. Published on May 31, 2011 as DOI: 10.1124/dmd.110.036467
This article has not been copyedited and formatted. The final version may differ from this version.

exclusion radiochromatogram of the guanidine-HCl treated 8 h female plasma sample. The radioactivity that eluted in the chromatographic region where the albumin standard eluted (between 10 and 20 min), was considered to be covalently bound to plasma proteins. The remainder of radioactivity which eluted from the size-exclusion column later than 30 min, in the chromatographic region where small molecules like GSK977779 elute, corresponded to unbound drug-related material. In male rat plasma, the amount of covalently bound radioactivity increased from 1.2% at 2 h post-dose to 30.8% at 24 h post-dose (Table 5). In female rat plasma the percentage of bound radioactivity increased from 23.8% at 2 h to 96.0% at 24 h post-dose (Table 5). The SEC results are in good agreement with the extractability data (Table 2) after accounting for the differences in overall recovery of sample radioactivity between the two methods. In addition, by comparison of the percent bound in Table 2 with the percent covalently bound in Table 5, it can be concluded that all of the non-extractable radioactivity was covalently bound.

SDS Gel Electrophoresis. Table 6 shows the percentage of plasma radioactivity retained on a polyacrylamide gel following SDS PAGE of male and female rat samples obtained from single oral dosing of [^{14}C]GSK977779 at 3 and 30 mg/kg. In male rat plasma at 30 mg/kg the amount of radioactivity retained on the gel increased from 1.3% at 2 h post-dose to 24% at 24 h. At the lower dose of 3 mg/kg in male rats the amount of plasma radioactivity retained on the gel was below the quantification limit of this technique. Following a dose of 3 mg/kg, in female rat plasma the amount of radioactivity retained on the gel was 35% at 2 h and increased to 92% at 24 h post dose. Similarly, at the dose of 30 mg/kg at the 2 h time point 16% of radioactivity was retained and increased to 78% at 24 h post dose. In all cases the retained radioactivity was detected

DMD Fast Forward. Published on May 31, 2011 as DOI: 10.1124/dmd.110.036467
This article has not been copyedited and formatted. The final version may differ from this version.

primarily in the gel sections where protein standards of 20-80 kDa were located including rat serum albumin (molecular weight: 64.3 kDa; Peters JR T, 1962). By comparison of the percent bound in Table 2 with the percent of radioactivity retained on the gel at the dose of 30 mg/kg in Table 6, it can be concluded that nearly 100% of the non-extractable radioactivity was covalently bound to plasma proteins.

Plasma Radioprofiles and Metabolites. Representative radio-HPLC chromatograms of reconstituted plasma extracts are depicted in Figure 4. Quantification of metabolites based on radio-HPLC is presented in Table 7. Chemical structures of identified [^{14}C]GSK977779 metabolites (including metabolites identified in plasma, urine or bile samples) are presented in Figure 7 and Figure 8 and of potential metabolites in Figure 9. In male rat plasma the major radiocomponent at all time points was the unchanged parent compound (55-99% of the extractable radioactivity). In female rat plasma, the parent compound was also the predominant radiocomponent at 2, 4 and 8 h post dose accounting for 69-94% of the extractable radioactivity. At 24 h the major radiocomponents were M23, which was tentatively identified as a conjugate of an amidine product of the reductive cleavage of the 1,2,4-oxadiazole ring, and a product of dehydrogenation, M35, which accounted for 50% and 24% of the extracted radioactivity, respectively. M14, a metabolite formed by reductive cleavage of the oxadiazole ring and subsequent conversion to a carboxylic acid was detected in male and female rat plasma at 2 (only in female) 4, 8, and 24 h post-dose and accounted for 1-11% of the extracted radioactivity. M4 (amidine), M11 and M12 (products of mono-oxygenation on the N-butyl chain), and M21 (another product of mono-oxygenation) were also detected in some male and female plasma samples.

DMD Fast Forward. Published on May 31, 2011 as DOI: 10.1124/dmd.110.036467
This article has not been copyedited and formatted. The final version may differ from this version.

Urine and Bile Radioprofiles and Metabolites. Representative radio-HPLC profiles of pooled rat urine samples after centrifugation are shown in Figure 5. Quantification of urine metabolites is presented in Table 8. Mass spectrometric analysis allowed for the identification of 76.1%, 88.6% and 78.3% of the radioactivity in intact male and female and BDC male urine samples, respectively. In male urine, the predominant metabolite was M9, a product of N-dealkylation, accounting for 33% of urinary radioactivity (5.8% of dose). Metabolites that resulted from cleavage of the 1,2,4-oxadiazole ring were M14, M4, M31 (mono-oxygenated cleavage product), M26 and M25 (mono-oxygenation plus dehydrogenation products of the amidine derivative), M1 and M2 (mono-oxygenated amidine derivatives), and M34 which together accounted for 35.3% of the urinary radioactivity (6.2% of dose). Additional metabolites were M12, M24, M21, M11 (products of mono-oxygenation) and M17 (product of di-oxygenation) which together accounted for 7.8% of the sample radioactivity (1.4% of dose). In pooled female urine, the major metabolites were M4 and M21, accounting for 21.8% and 26% of the urine radioactivity, respectively (or 6.9 and 8.14% of the dose, respectively). The metabolites which were products of oxadiazole ring cleavage, M4, M14, M34, M31, M25, M26, M2 and M1, accounted for 51.1% of the urinary radioactivity (16.2% of dose). The remainder of the identified metabolites, M21, M12 and M11 accounted for 36.6% of the sample radioactivity (11.5% of dose). An additional metabolite, M32, was detected in female urine by mass spectrometry, but was not quantifiable by radio-HPLC. This metabolite was a product of oxadiazole ring cleavage plus di-oxygenation and dehydrogenation (possibly a carboxylic acid). In both male and female urine only small

amounts of unchanged GSK977779 were detected. The metabolic profile of the BDC male urine was very similar to the profile of the intact male urine sample.

Figure 6 shows the metabolic profile of male BDC rat bile sample. Quantification of biliary metabolites is presented in Table 9. In bile the metabolites derived from oxadiazole ring cleavage (M4 and M14) accounted for 9.7% of the dose (assuming M4 accounted for the entire radioactivity under the peak where M5 and M17 co-eluted). The products of N-dealkylation, mono-oxygenation and dioxygenation (M9, M12, M21, M11 and M17) accounted together for at least 20.5% of the dose (without including M17 which co-eluted with M4 and M5). Additional metabolites identified in bile were: M5, a product of dechlorination, oxidation followed by opening of the fused imidazole ring and glucuronidation, M10 and M27 (mono-oxygenation plus glucuronidation), M28 (di-oxygenation), M29 and M30 (mono-oxygenation plus dechlorination plus glutathione conjugation) and M33 (oxidative dechlorination) which together accounted for approximately 10.6% of the dose; Metabolites M19 and M22 accounted for 0.8% and 0.3% of the dose, respectively and based on their mass spectra (Table 10) were identified as a product of di-oxygenation plus dehydrogenation and a product of mono-oxygenation, respectively. These minor metabolites with undefined positions of biotransformation were not included in Figure 7 or Table 9.

Identification of Metabolites by LC-MS/MS and NMR. Metabolite structures were elucidated by LC-MS and NMR analysis. Summaries of LC-MS^n and ^1H NMR data are depicted in Table 10, and Table 11, respectively. Figure 10 shows the NMR numbering schemes utilized for GSK977779 and its metabolites. The LC-MS data provided a Markush structure for the metabolites and further definitive structures on

DMD Fast Forward. Published on May 31, 2011 as DOI: 10.1124/dmd.110.036467
This article has not been copyedited and formatted. The final version may differ from this version.

selected metabolites were determined by NMR analysis of isolated metabolites. The MS and NMR structural assignments of the observed circulating metabolites as well as of metabolites M9 and M5 are discussed below. All MS discussion of the pseudo molecular ion and its fragments concern positive $[M+H]^+$ ions and the reported accurate mass measurements are within 5 ppm or 2 mDa of the theoretical mass.

Metabolite M9. The pseudo molecular ion at *m/z* 388 was 56 Da lower than GSK977779, with accurate mass indicating N-dealkylation. The MS^2 fragments at *m/z* 202 and 187 are assigned to the two ions resulting from the cleavage of the C-N bond located between the xanthine and bridging butyl moieties. Two distinct ^1H spin systems were observed in the NMR data. Upon comparison to those observed with GSK977779, these were assigned to the pyridine ring and the butyl chain which links the oxadiazole and xanthine moieties. The notable disappearance of the n-butyl ^1H NMR signals led to the proposed definitive structure.

Metabolite M11. The pseudo molecular ion at *m/z* 460 was 16 Da higher than GSK977779 with accurate mass indicating mono-oxygenation. MS^2 fragment ions at *m/z* 202 and 187 again show the unchanged oxadiazole pyridine containing the linking butyl chain and chlorinated xanthine moieties, respectively. The fragments at *m/z* 442 and 388 show a loss of water and loss of butanol, respectively, and place the site of biotransformation on the n-butyl chain. Three distinct ^1H spin systems were observed in the NMR data. Upon comparison to those observed with GSK977779, two of which may be assigned to the pyridine ring and the butyl chain which links the oxadiazole and xanthine moieties. The disappearance of the aliphatic methyl signal in conjunction with

the appearance of a new two-proton signal at 3.45 ppm implicate C13 as the site of biotransformation.

Metabolite M12. The observed pseudo molecular ion and MS^2 fragment ions were identical to those observed for metabolite M11, indicating a separate mono-oxygenation of GSK977779 on the same n-butyl chain. Similarly, two of the three distinct ^1H spin systems observed were assigned to the pyridine ring and the butyl chain which links the oxadiazole and xanthine moieties. The aliphatic methyl signal (shifted downfield 0.25 ppm to 1.06 ppm) was coupled to a CH moiety at 3.68 ppm identifying C12 as the site of biotransformation.

Metabolite M14. The pseudo molecular ion at *m/z* 343 was 101 Da lower than GSK977779. The accurate mass MS^2 product ions at *m/z* 297 and 243 indicate losses of formic acid and pentanoic acid from the chlorinated xanthine moiety, respectively. Two distinct ^1H spin systems were observed in the NMR data. Upon comparison to those observed with GSK977779, these may be assigned to the n-butyl side chain and the butyl chain which links the oxadiazole and xanthine moieties. The notable absence of the pyridinyl ring ^1H NMR signals led to the proposed definitive structure.

Metabolite M4. The pseudo molecular ion at *m/z* 341 was 103 Da lower than GSK977779. Accurate mass of the MS^2 fragment ion *m/z* 324 corresponded to the loss of ammonia. Fragments at *m/z* 243 and 99 were assigned as ion pairs from the C-N cleaveage between the chlorinated xanthine moiety and pentamidine, respectively. The remaining MS^2 fragment ions *m/*z 268 and 187 are loss of ammonia plus N-butyl dealkylation and dual N-dealkylations of the chlorinated xanthine, respectively,

indicating one unmodified butyl chain. These fragment ion assignments support the proposed amidine structure shown in Figure 7.

Metabolite M21. The pseudo molecular ion at *m/z* 460 was 16 Da higher than GSK977779 indicating mono-oxygenation by accurate mass. The MS^2 fragment ion at *m/z* 442 corresponded to the loss of water. The site of biotransformation was narrowed to the bridging butyl chain from the observation of two key MS^2 product ions: *m/z* 313 which corresponds to the loss of the oxadiazole pyridinyl moiety and *m/z* 200 which was assigned to the dehydrated butyl oxadiazole pyridinyl moiety. Together these fragment ions implicate the bridging butyl chain as the source of the observed MS^n water loss.

Metabolite M23. The pseudo molecular ion at m/z 470 was 26 Da higher than GSK977779. The MS2 fragmentation produced only three significant ions (m/z 425, 324, and 130) and was insufficient for definitive structural elucidation. However, the observation of the fragment ion at m/z 324 suggested that M23 may be a conjugate of metabolite M4 (M4+129 Da). The limited number of fragments as well as the low intensity of the fragment ions which limits the mass accuracy, only allow a tentative structural assignment.

Metabolite M35. The pseudo molecular ion at *m/z* 442 was 2 Da lower than GSK977779, indicating a net loss of two protons by accurate mass. The fragment ion at *m/z* 200 is the butyl oxadiazole pyridinyl moiety and the fragment at *m/z* 295 is the opposing side containing the bridging butyl and xanthine moeity. These accurate mass fragments both show a net loss of two protons and narrow the site of biotransformation to the bridging butyl chain.

DMD Fast Forward. Published on May 31, 2011 as DOI: 10.1124/dmd.110.036467
This article has not been copyedited and formatted. The final version may differ from this version.

Metabolite M5. The pseudo molecular ion at *m/z* 620 was 176 Da higher than GSK977779, absent of the Cl isotope pattern, and had accurate mass indicating glucuronidation. MS^2 fragment ions at *m/z* 603, 444, and 427 correspond to the loss of ammonia, loss of glucuronide, and loss of both, respectively. Four distinct ^1H spin systems were observed in the NMR data. Upon comparison to those observed with GSK977779, three of which may be assigned to the pyridine ring, the butyl chain which links the oxadiazole and xanthine moieties, and the n-butyl side chain. The fourth ^1H spin system is consistent with the presence of a glucuronic acid moiety. The ^{13}C chemical shift for the anomeric carbon at 103.4 ppm is indicative of an O-glucuronide.

Solubilization and Analysis of Plasma Protein Pellet. Figure 11 shows the radioprofile of the alkali hydrolysate of the protein pellet remaining after the extraction of the 24 h female plasma sample. Most of the sample radioactivity eluted as a single radioactive peak at retention time of 44.17 min. Similar results (the same major radiocomponent) were obtained following the solubilization and analysis of the 24 h male plasma protein pellet. The identity of the major radiocomponent was initially assigned based on its HPLC retention time as the carboxylic acid derivative of the 1,2,4-oxadiazole ring cleavage, metabolite M14. Following a subsequent experiment which involved dosing of non-radiolabelled GSK977779 to female rats and analysis of the 24 h plasma protein pellet, the identity of the only drug related component detected in the alkaline hydrolyzate of the pellet was confirmed by LC-MS/MS to be metabolite M14.

GSK977779 when incubated overnight at 50°C with 1M NaOH under the conditions described in the experimental section was found to slowly convert to a degradant which was identified by LC-MS/MS as the N-hydroxy derivative of the

amidine M4. The estimated amount of GSK977779 which degraded over the course of 19 hours was approximately 13% based on comparison of UV peak areas between the degradant and GSK977779 and assuming equal molar absorptivities at 278 nm. The hydrolytic decomposition of the 1,2,4-oxadiazole ring to yield the N-hydroxyamidine in the presence of acid or base has been observed earlier by several investigators (Paoloni and Cignitti, 1968; Tyrkov, 2001). This experiment indicated that the oxadiazole ring is relatively stable under the conditions of the pellet solubilization experiment and therefore provided us with some degree of confidence that M14 was not an artifact of the harsh conditions used to solubilize the protein pellet.

DMD Fast Forward. Published on May 31, 2011 as DOI: 10.1124/dmd.110.036467
This article has not been copyedited and formatted. The final version may differ from this version.

Discussion

As indicated by the biliary and urinary metabolic profiles GSK977779 was extensively metabolized in the rat by the following pathways: N-dealkylation, mono-oxygenation and di-oxygenation, reductive or oxidative cleavage of the oxadiazole ring and conjugative pathways observed mostly in bile. The metabolic profiles in plasma and urine were qualitatively similar, but quantitatively different between male and female rats as is often the case based on the established gender differences in expression levels of CYP and other biotransformation enzymes in this species (Robertson et al., 1998; Pampori and Shapiro, 1996). Overall, the higher metabolism of the parent molecule observed in female rat is consistent with the observation of higher levels of covalent binding in this gender.

During the sample preparation of rat plasma for metabolite profiling high amounts of non-extractable radioactivity were observed, particularly in female rats. Although there is no absolute threshold over which the concentration of non-extractable radioactivity can be linked with reactive metabolite formation and potential toxicity liabilities, the amount observed with [^{14}C]GSK977779 exceeded by far the tentative threshold of 50 pmol/mg which has been proposed by other investigators for in vitro or in vivo screening of drug candidates (Evans et al., 2004). Extractability was also measured in male and female rat liver samples and was found to be high relative to plasma. The higher covalent binding observed in plasma may indicate that the main site of bioactivation could be other than the liver (e.g., the intestine) and/or that the transport properties of the protein complex are favoring the plasma. Following incubation of [^{14}C]GSK977779 with rat and human liver microsomes the amount of NADPH-

DMD Fast Forward. Published on May 31, 2011 as DOI: 10.1124/dmd.110.036467
This article has not been copyedited and formatted. The final version may differ from this version.

dependent microsomal protein binding of radioactivity indicated the potential for bioactivation of [^{14}C]GSK977779. In the rat in vitro systems the NADPH-dependent covalent binding was higher in female than in male, while in human liver microsomes there was no significant difference between the two sexes suggesting that the sex differences could be species specific (Skett, 1988). The observation of high plasma non-extractable radioactivity led to further investigation of the reversibility of the observed binding. SEC and SDS PAGE have been used in the past to investigate the covalent versus non-covalent binding to plasma proteins (Eling et al., 1977; Zhou et al., 1996; Walsh et al., 2002). SEC and SDS PAGE of selected plasma samples from rats dosed with [^{14}C]GSK977779 showed that the non-extractable radioactivity was covalently bound to plasma proteins. Both the co-chromatography of radioactivity with the albumin standard in SEC and the appearance of radioactivity primarily in the 20-80 kDa gel sections following SDS PAGE indicated that the bound radioactivity was primarily associated with albumin. The evidence of extensive covalent binding of [^{14}C]GSK977779-related radioactivity suggests that the molecule undergoes bioactivation in rats to one or more reactive metabolites which covalently bind to protein residues. Reactive metabolites are usually short-lived intermediates which are hard to detect in the plasma extracts or in the precipitated plasma protein. However, the identification of the metabolites of the drug-candidate by LC-MS/MS and NMR analysis of plasma and excreta samples may provide indirect evidence regarding the reactive pathway and a basis to propose a mechanism(s) leading to covalent binding. In addition, alkaline hydrolysis of the protein pellet which achieves its solubilization and the release of the bound

radioactivity, occasionally allows for the characterization of the structure of the bound metabolite(s) (Bailey and Dickinson, 1996).

It has been reported that the biotransformation of the 1,2,4-oxadiazole can proceed by reductive cleavage to generate amidine, amide, diamide and carboxylic acid derivatives (Lan et al., 1973; Speed et al., 1994; Ulrich et al. , 2001; Bateman et al., 2006). An oxidative cleavage pathway which leads to the formation of a cyanamide has also been reported by Yabuki et al., 1993, and Bateman et al., 2006. In the present report, based on the nature of the identified metabolites, we speculate that the oxadiazole ring is cleaved via both reductive and oxidative mechanisms with the former being more prominent. Figure 7 shows the proposed phase I biotransformation pathways of [^{14}C]GSK977779 in rats including a tentatively identified conjugate of M4 detected in plasma. The metabolites M4, M1, M2, M25, M26, M23, M14 and M34 are products of reductive cleavage and M31, M32 products of oxidative cleavage of the oxadiazole ring. Figure 8 shows the Phase II metabolites of [^{14}C]GSK977779 detected only in rat bile. Complete elucidation of the products of the oxadiazole ring cleavage could not be achieved due to the position of the radiolabel. However, the identification of the cleavage products that retained the radiolabel in their structure allowed us to propose the structure of the metabolites derived from the other half of the molecule. In the case of the oxidative cleavage of the oxadiazole ring metabolites M32 and M31 provided indirect evidence for the formation of the pyridinecarboxylic acid cyanamide. Other putative products of the reductive cleavage of GSK977779 would be the pyridinocarboxylic acid or the pyridine carboxylic acid amide. Figure 9 displays the structures of the above three putative metabolites.

DMD Fast Forward. Published on May 31, 2011 as DOI: 10.1124/dmd.110.036467
This article has not been copyedited and formatted. The final version may differ from this version.

Oxadiazole ring metabolism has been studied by many investigators, however, to our knowledge, its implication with covalent binding has not been documented in the literature before. Oxamide resulting from cleavage of oxadiazole ring has been reported to be responsible for long-lived radioactivity in dog plasma but according to the authors, there was no evidence for covalent binding of oxamide to plasma protein (Allan et al., 2006). In the case of GSK977779, several metabolite structures raised reactive metabolite alerts including the products of the reductive cleavage of the oxadiazole ring (the amidine, M4, and its mono-oxygenated derivatives, M1 and M2, metabolites M25 and M26, the unidentified conjugate, M23 and the carboxylic acid, M14), the product of oxadiazole ring cleavage and dehydrogenation M34, metabolite M32 (possibly deriving from oxidative cleavage of the oxadiazole and carboxylic acid formation), the glutathione conjugates (M29 and M30) and metabolite M5, an acyl glucuronide. The detection of M4, M23 and the other amidine derivatives suggested that the amidine group could potentially form a conjugate with a carboxyl group from a macromolecule. Amidine groups can form non-covalent, hydrogen bonds with carboxyl groups of macromolecules (Peters et al., 2001). Such bonds should be disrupted by treatment with 6M guanidine hydrochloride (Peters et al., 2001). Our SEC experiments showed that the [^{14}C]GSK977779-related radioactivity remained bound to protein even after 6M guanidine treatment suggesting the irreversible nature of the binding through a mechanism other than an amidine-carboxylic acid hydrogen bond. Covalent binding could also occur from the addition of a cysteine group of a macromolecule on an alkene intermediate in a Michael fashion. This type of reaction is usually observed in the presence of an electron withdrawing group adjacent to the double bond (Kalgutkar and

DMD Fast Forward. Published on May 31, 2011 as DOI: 10.1124/dmd.110.036467
This article has not been copyedited and formatted. The final version may differ from this version.

Soglia, 2005). Such an example exists for M34 which may contain a double bond at a α-position to the carboxyl group. The results of the in vitro GSH trapping experiment, where no GSK977779-related glutathione adduct was detected, indicated that the addition of a cysteine group of a macromolecule to an alkene containing metabolite of GSK977779 was not the likely pathway leading to covalent binding with this molecule. In vivo, the glutathione conjugates M29 and M30 which were detected at low levels in rat bile, were products of nucleophilic substitution of the chlorine atom. Indirect evidence that this pathway was not the predominant pathway leading to covalent binding was provided from in vivo experiments with another molecule, compound BA with structural similarities to GSK977779 (Figure 12). This compound which contained the same substituted purine ring and differed from GSK977779 only in the composition of the R group (left part of the molecule) did not demonstrate any covalent binding after dosing to rats.

In order to release the covalently bound moiety of GSK977779, the precipitated protein samples from the 24 h male and female plasma were treated with alkali to hydrolyze the amino acid backbone and potentially the covalent bond with the drug. The chromatographic analysis of the solubilized protein yielded one major peak which was identified as metabolite M14. It is possible that the harsh alkali treatment of the protein pellet had altered the structure of the bound metabolite.

Overall, based on the above experiments we cannot claim that we positively identified the covalently bound moiety to plasma protein. However, the results of the glutathione trapping assay as well as the abolishment of covalent binding by replacement of the oxadiazole ring in compound BA suggested that one or more products of the

oxadiazole ring cleavage resulted to the observed covalent binding with GSK977779. In addition, the analysis of the solubilized plasma protein pellet further suggested the possibility that the bound moiety could be the carboxylic acid M14 or a derivative thereof. A number of carboxylic acids have been associated with adverse reactions linked to the metabolic activation through formation of acyl glucuronides or acyl-CoA esters (Skonberg et al., 2008). In the case of GSK977779 covalent binding could have resulted from further bioactivation of M14 by formation of an acyl glucuronide or an acyl-CoA ester. However, such metabolites have not been detected in rat plasma or other matrices, possibly due to their high reactivity.

The finding of extensive covalent binding of drug-related material to plasma or liver protein during the in vivo ADME studies in preclinical species constitutes an alert for potential for idiosyncratic toxicity that together with other factors such as the dose level, the anticipated duration of the treatment and the severity of the indication should guide the risk assessment for the drug candidate. In the case of GSK977779 the molecule initially did not raise any structural alerts, was found to be non-genotoxic based on in vitro and in vivo genotoxicity testing and was well tolerated in a 7-day repeat dose toxicity study in the rat. However, the finding of extensive covalent binding in rats contributed to the termination of this candidate from progression to human trials. Further investigations regarding the identity of the covalently bound metabolite could be performed using enzyme digestion of the isolated protein adduct or MALDI MS to analyze the plasma protein-GSK977779-related adduct. This research would be of broad interest to the pharmaceutical community since the oxadiazole ring is commonly used in place of ester linkages in the structures of xenobiotics (Watjen et al., 1989).

Acknowledgements. The authors thank Drs. Cosette Serabjit-Singh, Gary Bowers, Giovanni Vitulli, Kitaw Negash, Tom Wilde, Hermes Licea-Perez, Steve Castellino, David Wagner, Mrs. Jill Pirhalla, Ms. Caroline Sychterz, Mr. Mike Morris, Ms. Laura Fotiou and Mr. John Ulicne for their scientific input and/or assistance in the preparation of the manuscript.

Authorship Contributions:

Participated in research design: Catherine Tsalta, Armina Madatian, Jennifer Seymour, Yanli Deng, Peter Gorycki

Conducted experiments: Armina Madatian, Jennifer Seymour, Ernest Schubert, Yanli Deng, Fangming Xia

Contributed new reagents or analytical tools: Not applicable

Performed data analysis: Catherine Tsalta, Armina Madatian, Jennifer Seymour, Ernest Schubert, Yanli Deng, William Hardesty, Fangming Xia

Wrote or contributed to the writing of the manuscript: Catherine Tsalta, Armina Madatian, Ernest Schubert, Yanli Deng, Peter Gorycki, William Hardesty, Fangming Xia

References

Allan GA, Gedge JI, Nedderman ANR, Roffey SJ, Small F, and Webster R (2006) Pharmacokinetics and metabolism of UK-383, 367 in rats and dogs: A rationale of long-lived plasma radioactivity. *Xenobiotica* **36:** 399-418.

Bailey MJ and Dickinson RG (1996) Chemical and immunochemical comparison of protein adduct formation of four carboxylate drugs in rat liver and plasma. *Chem Res Toxicol* **9**: 659-666.

Bateman KP, Trimble L, Chauret N, Silva J, Day S, Macdonald D, Dube D, Gallant M, Mastracchio A, Perrier H, Girard Y, and Nicoll-Griffth D (2006) Interspecies *in vitro* metabolism of the phosphodiesterase-4 (PDE4) inhibitor L-454, 560. *J Mass Spectrom* **41:** 771-780.

Davies B and Morris T (1993) Physiological parameters in laboratory animals and humans. *Pharm Res* **10:** 1093-1095.

Eling TE, Wilson AGE, Chaudhuri A, and Anderson MW (1977) Covalent binding of an intermediate(s) in prostaglandin biosynthesis to guinea pig lung microsomal protein. *Life Sciences* **21:** 245-252.

Evans DC, Watt AP, Nicoll-Griffith DA, and Baillie TA (2004) Drug-protein adducts: an industrial perspective on minimizing the potential for drug bioactivation in drug discovery and development. *Chem Res Toxicol* **17:** 3-16.

Fuccella LM, Goldaniga G, Lovisolo P, Maggi E, Musatti L, Mandelli V, and Sirtori CR (1980) Inhibition of lipolysis by nicotinic acid and by acipimox. *Clin Pharmacol Ther* **28:** 790-795.

Grundy SM, Mok HYI, Zech L, and Berman M (1981) Influence of nicotinic acid on metabolism of cholesterol and triglycerides in man. *J Lipid Res* **22:** 24-36.

Kalgutkar AS and Soglia JR (2005) Minimising the potential for metabolic activation in drug discovery. *Expert Opin Drug Metab Toxicol*. **1**: 91-142.

Karpe F and Frayn KN (2004) The nicotinic acid receptor-a new mechanism for an old drug. *Lancet* **363:** 1892-1894.

Lan SJ, Weliky I, and Schreiber EC (1973) Metabolic Studies with *Trans*-5-Amino-3-[2-(5-Nitro-2-Furyl)Vinyl]-1,2,4-[5-^{14}C]Oxadiazole (SQ 18,506): 1. Reductive Cleavage of the 1, 2, 4-oxadiazole ring. *Xenobiotica* **3**: 97-102.

Pampori NA and Shapiro BH (1996) Feminization of hepatic cytochrome P450s by nominal levels of growth hormone in the feminine plasma profile. *Mol Pharmacol* **50:** 1148-1156.

Paoloni L and Cignitti M (1968) Electronic structure and chemical properties of 1,2,4-oxadiazole, bis-1,2,4-oxadiazoles and other derivatives. *Tetrahedron* **24**: 485-489.

Peters L, Frohlich R, Boyd ASF, and Kraft A (2001) Tetrazole binding to amidine bases. *Fifth International Electronic Conference on Synthetic Organic Chemistry (ECSOC-5):* 1-10.

Peters JR T (1962) The Biosynthesis of rat serum albumin. III. Amino acid composition of rat albumin. *J Biol Chem* **237:** 2182-2183.

Robertson GR, Farrell GC, and Liddle C (1998) Sexually dimorphic expression of rat CYP3A9 and CYP3A18 genes is regulated by growth hormone. *Biochem Biophys Res Commun* **242:** 57-60.

Saadane A, Neveux N, Feldmann G, Lardeux B, and Bleiberg-Daniel F (1996) Inhibition of liver RNA breakdown during acute inflammation in the rat. *Biochem J* **317**: 907-912.

Skett P (1988) Biochemical basis of sex differences in drug metabolism. *Pharmac Ther* **38**: 269-304.

Skonberg C, Olsen J, Grimstrup M, Hansen SH, and Grillo MP (2008) Metabolic activation of carboxylic acids. *Expert Opin Drug Metab Toxicol* **4**: 425-438.

Speed W, Parton AH, Martin IJ, and Howard MR (1994) The use of liquid chromatography/thermospray mass spectrometry with online ultraviolet diode array and radiochemical detection: characterization of the putative metabolites of U-78875 in female rat feces. *Biol Mass Spectom* **23:** 1-5.

Tunaru S, Kero J, Schaub A, Wufka C, Blaukat A, Pfeffer K, and Offermanns S (2003) PUMA-G and HM74 are receptors for nicotinic acid & mediate its anti-lipolytic effect. *Nat Med* **9:** 352-355.

Tyrkov AG (2001) Acid hydrolysis of 3-aryl-5-trinitromethyl-1,2,4-oxadiazoles. *Russ J Org Chem* **37**:1353-1354.

Ulrich RG, Bacon JA, Brass EP, Cramer CT, Petrella DK, and Sun EL (2001) Metabolic, idiosyncratic toxicity of drugs: overview of the hepatic toxicity induced by the anxiolytic, panadiplon. *Chem Biol Interact* **134:** 251-270

Walsh JS, Reese MJ, and Thurmond LM (2002) The metabolic activation of abacavir by human liver cytosol and expressed human alcohol dehydrogenase isozymes. *Chem Biol Interact* **142:** 135-154.

Watjen F, Baker R, Engelstoff M, Herbert R, MacLeod A, Knight A, Merchant K, Moseley J, Saunders J, Swain CJ, Wong E, and Springer JP (1989) Novel benzodiazepine receptor partial agonists: Oxadiazolylimidazobenzodiazepines. *J Med Chem* **32:** 2282-2291.

Wise A, Foord SM, Fraser NJ, Barnes AA, Elshourbagy N, Eilert M, Ignar DM, Murdock PR, Steplewski K, Green A, Brown AJ, Dowell SJ, Szekeres PG, Hassall DG, Marshall FH, Wilson S, and Pike NB (2003) Molecular identification of high and low affinity receptors for nicotinic acid. *J Biol Chem* **278:** 9869-9874.

Yabuki M, Shono F, Nakatsuka I, and Yoshitake A (1993) Novel cleavage of the 1,2,4-oxadiazole ring in rat metabolism of SM-6586, a dihydropyridine calcium antagonist. *Drug Metab Dispos* **21:**1167-1169.

Yan Z, Easterwood LM, Maher N, Torres R, Huebert N, and Yost GS (2007) Metabolism and bioactivation of 3-methylindole by human liver microsomes. *Chem Res Toxicol* **20**: 140-148.

Zhou L, McKenzie BA, Eccleston Jr. ED, Srivastava SP, Chen N, Erickson RR, and Holtzman JL (1996) The covalent binding of [14C]acetaminophen to mouse hepatic microsomal proteins: The specific binding to calreticulin and the two forms of the thiol:protein disulfide oxidoreductases. *Chem Res Toxicol* **9:** 1176-1182.

Legends for Figures

Figure 1. Chemical structure of [^{14}C]GSK977779. The asterisk denotes the position of C-14.

Figure 2. UV chromatogram of rat serum albumin (0.9 mg/ml) and GSK977779 (0.05 mg/ml) standards at 280 nm following denaturation with 6M guanidine-HCl and size-exclusion chromatography on a BioSep-SEC-S3000 column.

Figure 3. Representative radiochromatogram of 8 h female rat plasma sample following denaturation with 6M guanidine-HCl and size-exclusion chromatography on a BioSep-SEC-S3000 column.

Figure 4. Representative metabolite radioprofiles of plasma extracts following a single oral administration of [^{14}C]GSK977779 to rats. Metabolite peaks representing less than 2% of the total plasma extract radioactivity are not discernible in this magnification scale of the radiochromatograms. P represents the parent compound. M followed by a number identifies uniquely one metabolite.

Figure 5. Representative metabolite radioprofiles of urine samples following a single oral administration of [^{14}C]GSK977779 to rats. P represents the parent compound. M followed by a number identifies uniquely one metabolite.

Figure 6. Representative metabolite radioprofile of bile sample following a single oral administration of [^{14}C]GSK977779 to bile duct-cannulated (BDC) rats. P represents the parent compound. M followed by a number identifies uniquely one metabolite.

Figure 7. Proposed phase I biotransformation pathways of [^{14}C]GSK977779 in rats including an unidentified conjugate detected in plasma. The position of the radiolabel is only shown in the parent compound structure.

Figure 8. Phase II metabolites of [^{14}C]GSK977779 detected in rat bile. The position of the radiolabel is only shown in the parent compound structure.

Figure 9. Putative chemical structures of [^{14}C]GSK977779 metabolites formed by cleavage of the oxadiazole ring but lacking the radiolabel in their structure.

Figure 10. NMR numbering schemes utilized for GSK977779 and its metabolites.

Figure 11. HPLC radioprofile of the alkali hydrolysate of plasma protein remaining after the extraction of the 24 h rat female plasma sample. The plasma sample was obtained from rats after a single oral dose of [^{14}C]GSK977779 at 30 mg/kg.

Figure 12. Chemical structure of compound BA.

DMD Fast Forward. Published on May 31, 2011 as DOI: 10.1124/dmd.110.036467
This article has not been copyedited and formatted. The final version may differ from this version.

Table 1

Mean recoveries of radioactivity following single oral administration of [^{14}C]GSK977779 (30 mg/kg) to Sprague Dawley rats

	Intact Males	Intact Females	BDC Male
Feces	73.3 ± 1.6	58.3 ± 2.5	19.8 ± 2.4
Urine	19.0 ± 1.2	33.0 ± 3.7	19.1 ± 3.0
Bile	NA	NA	52.1 ± 4.6
Total [a]	93.3 ± 0.4	93.5 ± 1.6	92.7 ± 0.4

Values are the mean ± standard deviation (n=3), where applicable

[a] Includes radioactivity recovered in cage rinse, wash, wipe and animal carcass

NA: Not applicable

DMD Fast Forward. Published on May 31, 2011 as DOI: 10.1124/dmd.110.036467
This article has not been copyedited and formatted. The final version may differ from this version.

Table 2

Extractable and non-extractable (bound) radioactivity in plasma samples following single oral administration of [^{14}C]GSK977779 (30 mg/kg) to male and female rats

Time Post Dose (h)	Sex	Total Drug-related Material[a] (µg eq/g)	% Extractable[b]	% Bound[c]	Bound[d] (pmol/mg protein)	% Total Recovery[e]
2	M	211	87.3	1.2	83.5	88.5
4	M	157	87.0	2.9	150	89.9
8	M	84	75.2	7.0	195	82.2
24	M	14	56.5	24.8	116	81.3
2	F	226	67.0	18.3	1366	85.3
4	F	149	40.7	43.3	2145	84.0
8	F	90	17.0	75.3	2228	92.3
24	F	44	6.3	81.9	1182	88.2

M: Male, F: Female

[a] Mean concentration of radioactivity (n=3) in plasma of males and females. All other data were obtained from pooled samples per sex across time points.

[b] Percent of total radioactivity recovered following solvent extraction.

[c] Percent of total radioactivity recovered after solubilization of the plasma protein pellets.

[d] Bound radioactivity expressed as pmol equivalent of GSK977779 per mg of plasma protein

[e] The sum of the percent extractable and the percent non-extractable.

DMD Fast Forward. Published on May 31, 2011 as DOI: 10.1124/dmd.110.036467
This article has not been copyedited and formatted. The final version may differ from this version.

Table 3

Extractable and non-extractable (bound) radioactivity in liver following single oral administration of [^{14}C]GSK977779 (30 mg/kg) to male and female rats

Time Post Dose (h)	Sex	Total Drug-related Material[a] (µg eq/g)	% Extractable[b]	% Bound[c]	Bound[d] (pmol/mg protein)	% Total Recovery
2	M	84.8	97.1	NA	NA	NA
4	M	67.4	98.1	NA	NA	NA
8	M	32.4	97.5	NA	NA	NA
24	M	6.8	90.7	NA	NA	NA
2	F	89.2	97.4	NA	NA	NA
4	F	64.0	95.5	NA	NA	NA
8	F	25.8	88.5	NA	NA	NA
24	F	8.9	85.1	14.9	18.4	100

M: Male, F: Female; NA: Not applicable

[a] Mean concentration of radioactivity (n=3) in liver of males and females. Extraction data were obtained from pooled samples per sex across time points.

[b] Percent of total radioactivity recovered following solvent extraction.

[c] Calculated percent of total non-extractable (bound) radioactivity assuming a sum of extractable plus non-extractable radioactivity equal to 100% for the female 24 h liver sample. No experimental determination of the bound radioactivity was done for any of the liver samples.

DMD Fast Forward. Published on May 31, 2011 as DOI: 10.1124/dmd.110.036467
This article has not been copyedited and formatted. The final version may differ from this version.

[d] Bound radioactivity expressed as pmol equivalent of GSK977779 per mg of liver protein.

DMD Fast Forward. Published on May 31, 2011 as DOI: 10.1124/dmd.110.036467
This article has not been copyedited and formatted. The final version may differ from this version.

Table 4

Amount of [^{14}C]GSK977779- or [^{14}C]Acetaminophen-related material bound to rat and human liver microsomal protein following incubation in the presence of NADPH

	Binding in the Presence of NADPH (pmol/mg)			
	Rat		Human	
Incubation Time (min)	30	60	30	60
GSK977779;M	72.2	177	86.3	136
Acetaminophen Control; M	NA[a]	75.8	NA	104
GSK977779; F	140	295	83.9	132
Acetaminophen control; F	NA	22.5	NA	158

M: male, F: female

[a] Not applicable; Acetaminophen control incubations were performed for 60 minutes only

DMD Fast Forward. Published on May 31, 2011 as DOI: 10.1124/dmd.110.036467
This article has not been copyedited and formatted. The final version may differ from this version.

Table 5

Unbound and covalently bound radioactivity in plasma samples measured by size exclusion chromatography after single oral administration of [^{14}C]GSK977779 (30 mg/kg) to male and female rats

Time Post Dose (h)	Sex	Total Drug-related Material[a] (µg eq/g)	% Unbound[b]	% Covalently Bound[c]	Total Recovery[d]
2	M	211	95.7	1.2	96.9
4	M	157	93.8	2.4	96.2
8	M	84.0	87.6	8.5	96.2
24	M	14.0	62.6	30.8	93.4
2	F	226	72.5	23.8	96.3
4	F	149	41.0	55.9	96.9
8	F	90.0	8.5	86.9	95.4
24	F	44.0	2.8	96.0	98.8

[a] Mean concentration of radioactivity (n=3) in plasma of males and females. All other data were obtained from pooled samples per sex across time points.

[b] Amount of radioactivity recovered in chromatographic region where small molecules eluted.

[c] Amount of radioactivity recovered in chromatographic region where albumin standard eluted.

[d] The sum of the percent unbound and percent covalently bound radioactivity.

DMD Fast Forward. Published on May 31, 2011 as DOI: 10.1124/dmd.110.036467
This article has not been copyedited and formatted. The final version may differ from this version.

Table 6

Amount of radioactivity retained on gel following electrophoresis of plasma samples obtained after single oral administration of [^{14}C]GSK977779 at 3 or 30 mg/kg to male and female rats

Time Post Dose (h)	Sex	Total Drug-related Material (µg/g)		Percent of Plasma Radioactivity Retained on Gel (mean ± SD)	
		3 mg/kg	30 mg/kg	3 mg/kg	30 mg/kg
2	M	18.0	159	BLQ	1.3 ± 0.1
24	M	1.74	16.2	BLQ	24 ± 4
2	F	10.2	152	35 ± 12	16 ± 3
24	F	2.62	28.4	92 ± 10	78 ± 3

BLQ: Below the limit of quantification

DMD Fast Forward. Published on May 31, 2011 as DOI: 10.1124/dmd.110.036467
This article has not been copyedited and formatted. The final version may differ from this version.

Table 7

Quantification of radiolabeled metabolites in plasma after single oral administration of [^{14}C]GSK977779 at 30 mg/kg to male and female rats

Parent or Metabolite	Percent of Total Radioactivity Recovered in Extract[a]							
	Intact Male				Intact Female			
	2h	4h	8h	24h	2h	4h	8h	24h
P	98.7	55.7	55.2	94.8	85.7	68.6	93.5	6.36
M4	ND	2.24	1.48	0.26	0.84	2.83	0.57	1.15
M11	ND	3.24	3.20	ND	0.50	1.79	0.38	NQ
M12	ND	12.1	13.2	ND	ND	2.46	0.19	1.15
M14	ND	10.5	10.8	0.80	1.73	7.23	2.67	4.05
M21	1.26	8.85	8.80	2.40	11.2	15.8	1.91	1.73
M23	ND	ND	ND	ND	ND	ND	ND	49.7
M35	ND	7.34	7.30	1.72	ND	1.25	0.76	24.3

ND: Not detected; NQ: Detected by mass spectrometry but not quantifiable by radio-HPLC

[a] Percent distribution of radioactivity under each identified peak

DMD Fast Forward. Published on May 31, 2011 as DOI: 10.1124/dmd.110.036467
This article has not been copyedited and formatted. The final version may differ from this version.

Table 8

Quantification of radiolabeled metabolites in urine after single oral administration of [^{14}C]GSK977779 at 30 mg/kg to male and female intact and BDC male rats

Parent or Metabolite Code	Mean Percent of Urine Radioactivity (Mean Percent of Administered Dose) [a]		
	Intact Male	Intact Female	BDC male
P	0.04 (0.01)	0.18 (0.05)	ND
M1	1.20 (0.21)	0.39 (0.12)	0.28 (0.05)
M2	0.72 (0.13)	0.74 (0.23)	0.28 (0.05)
M4	12.8 (2.22)	21.8 (6.90)	12.8 (2.11)
M9	33.0 (5.80)	ND	32.9 (5.63)
M11	0.58 (0.10)	0.81 (0.25)	1.12 (0.19)
M12	3.31 (0.58)	9.79 (3.07)	1.35 (0.22)
M14	13.4 (2.37)	8.21 (2.58)	21.1 (3.56)
M17	1.87 (0.33)	0.67 (0.20)	2.23 (0.38)
M21	0.68 (0.12)	26.0 (8.14)	1.35 (0.22)
M24	1.32 (0.24)	ND	1.50 (0.25)
M25	1.38 (0.24)	4.83 (1.55)	0.58 (0.11)
M26	3.36 (0.59)	3.85 (1.22)	1.89 (0.35)
M31	1.91 (0.34)	5.65 (1.80)	0.88 (0.16)
M34	0.51 (0.09)	5.65 (1.76)	ND

DMD Fast Forward. Published on May 31, 2011 as DOI: 10.1124/dmd.110.036467
This article has not been copyedited and formatted. The final version may differ from this version.

Total Quantified [b]	76.1 (13.3)	88.6 (27.9)	78.3 (13.3)

ND: Not detected

[a] Mean percent radioactivity recovered under each peak also expressed as percent of the administered dose in parenthesis

[b] Total quantified represents the percentage of urine sample radioactivity that was assigned structures expressed also as percent of the administered dose

DMD Fast Forward. Published on May 31, 2011 as DOI: 10.1124/dmd.110.036467
This article has not been copyedited and formatted. The final version may differ from this version.

Table 9

Quantification of radiolabeled metabolites in bile after single oral administration of [^{14}C]GSK977779 at 30 mg/kg BDC male rats

Parent or Metabolite Code	Mean Percent of Bile Radioactivity (Mean Percent of Administered Dose)
P	0.12 (0.07)
M4, M5, M17 [a]	13.6 (6.98)
M9	23.1 (12.0)
M10	4.56 (2.29)
M11	3.61 (1.87)
M12	7.27 (3.71)
M14	5.24 (2.68)
M21	5.56 (2.91)
M27, M28 [a]	9.57 (4.91)
M29	2.27 (1.17)
M30	2.19 (1.14)
M33	2.11 (1.08)
Total Quantified	79.2 (40.8)

[a] Co-elution of metabolites M4, M5 and M17 and metabolites M27 and M28 was observed with the HPLC method used.

DMD Fast Forward. Published on May 31, 2011 as DOI: 10.1124/dmd.110.036467
This article has not been copyedited and formatted. The final version may differ from this version.

Table 10

Selected mass spectra data for GSK977779 and its metabolites

Metabolite	*m/z*	
	$[M+H]^+$	Significant MS^2 and MS^3 Product Ions[a]
GSK977779	444	MS^2: 365, 322, 297, 255, 243, 202, 187, 170, 106
M1	357	MS^2: 322, 280, 268, 198, 187, 156, 144
M2	357	MS^2: 322, 280, 268, 198, 187, 156, 144
M4	341	MS^2: 324 268, 243, 200, 187, 170, 144, 99
M5	620	MS^2: 603, 444, 427
M9	388	MS^2: 266, 202, 199, 187, 170
M10	636	MS^2: 460, 444; MS^3 on 460: 443, 313 [b]
M11	460	MS^2: 442, 400, 388, 295, 253, 245, 241, 202, 199, 187
M12	460	MS^2: 442, 400, 388, 295, 253, 245, 241, 202, 199, 187
M14	343	MS^2: 297, 255, 243, 199, 187, 170
M17	476	MS^2: 458 ; MS^3 on 458: 440, 386, 311, 241, 200, 187 [b]
M19	474	MS^2: 456, 428, 309, 245, 212, 202
M21	460	MS^2: 442; 313, 295, 255, 243, 200, 187
M22	460	MS^2: 443; 313, 271, 259, 203, 202, 188, 106
M23	470	MS^2: 425, 324, 130
M24	460	MS^2: 442, 388, 295, 241, 202, 187
M25	355	MS^2: 337; MS^3 on 337: 320, 243, 187, 169, 95 [c]
M26	355	MS^2: 337; MS^3 on 337: 320, 243, 187, 169, 95 [c]

DMD Fast Forward. Published on May 31, 2011 as DOI: 10.1124/dmd.110.036467
This article has not been copyedited and formatted. The final version may differ from this version.

Metabolite	*m/z*	
	$[M+H]^+$	Significant MS^2 and MS^3 Product Ions[a]
M27	636	MS^2: 460, 442, 202
M28	476	no MS^n data
M29	731	MS^2: 713, 585, 458, 274, 199, 145
M30	731	MS^2: 713, 585, 458, 274, 199, 145
M31	315	MS^2: 297; MS^3 on 297: 255, 243, 241 [b]
M32	329	MS^2: 311; MS^3 on 311: 283, 255, 243, 227, 199, 187, 169 [c]
M33	426	MS^2: 304, 279, 248, 237, 225, 202, 169, 123, 106
M34	341	MS^2: 323, 295, 281, 243, 239, 225, 187
M35	442	MS^2: 414, 320, 295, 239, 200, 106

[a] Major or significant positive product ions. Unless otherwise noted, reported MS fragments were acquired on a Waters QToF II.

[b] MS^n data from Thermo LTQ

[c] Species exhibited significant in-source fragmentation. The dominant in-source fragment ion ($-H_2O$) is labeled MS^2 and was used to generate additional fragments (MS^3).

DMD Fast Forward. Published on May 31, 2011 as DOI: 10.1124/dmd.110.036467
This article has not been copyedited and formatted. The final version may differ from this version.

Table 11

^{1}H NMR data for GSK977779 and selected metabolites [a]

Atom	GSK977779	M5	M9	M11	M12	M14
10	3.88	3.67 & 3.78	•	3.88	3.92 & 3.96	3.89
11	1.56	1.48	•	1.62	1.65 & 1.73	1.58
12	1.24	1.18	•	1.45	3.68	1.26
13	0.81	0.78	•	3.45	1.06	0.84
14	3.91	3.87	3.87	3.91	3.91	3.84
15	1.63	1.63	1.63	1.63	1.63	1.50
16	1.73	1.74	1.74	1.74	1.74	1.51
17	2.79	2.81	2.80	2.80	2.80	2.18
23	8.12	8.17	8.14	8.13	8.13	•
24	8.00	8.02	8.01	8.01	8.01	•
25	7.62	7.62	7.62	7.62	7.62	•
26	8.68	8.68	8.68	8.68	8.68	•
27	•	4.61	•	•	•	•
28	•	3.37	•	•	•	•
29	•	3.38	•	•	•	•
30	•	3.38	•	•	•	•
31	•	3.53	•	•	•	•

[a] Data acquired in 1:1 (v/v) acetonitrile-d_3:D_2O; values are chemical shifts in ppm

Figure 1

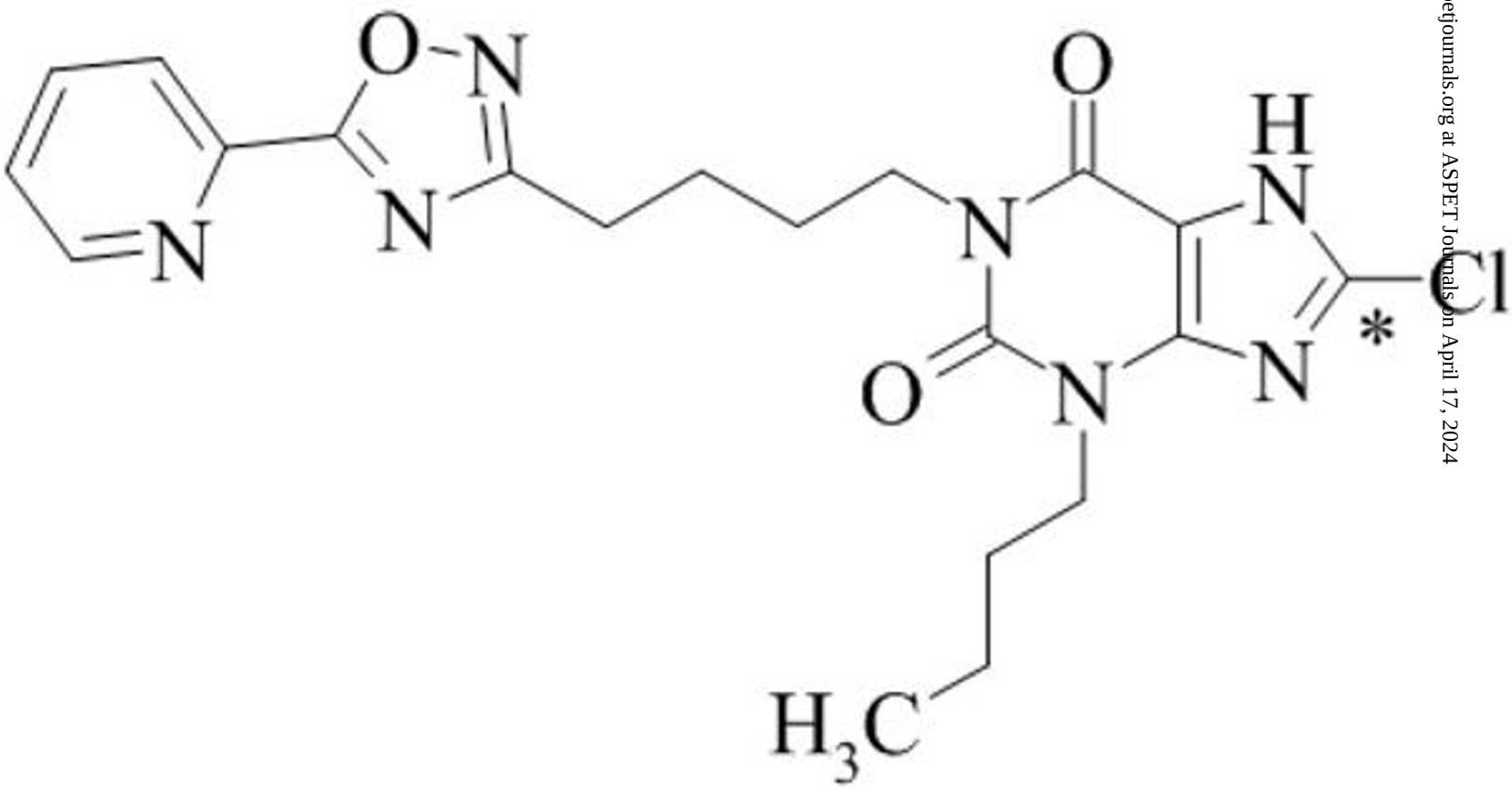

[^{14}C]GSK977779

Figure 2

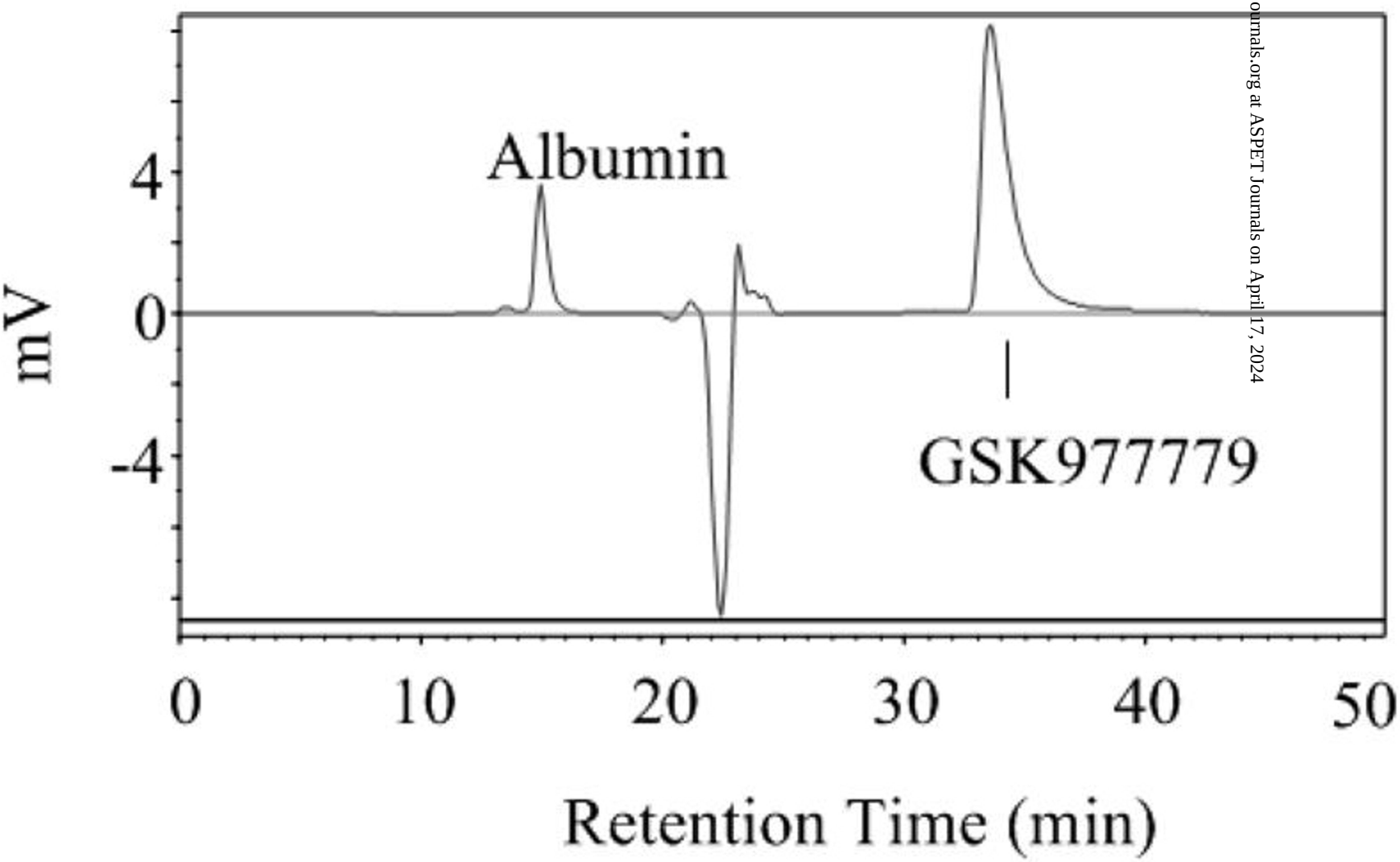

Figure 3

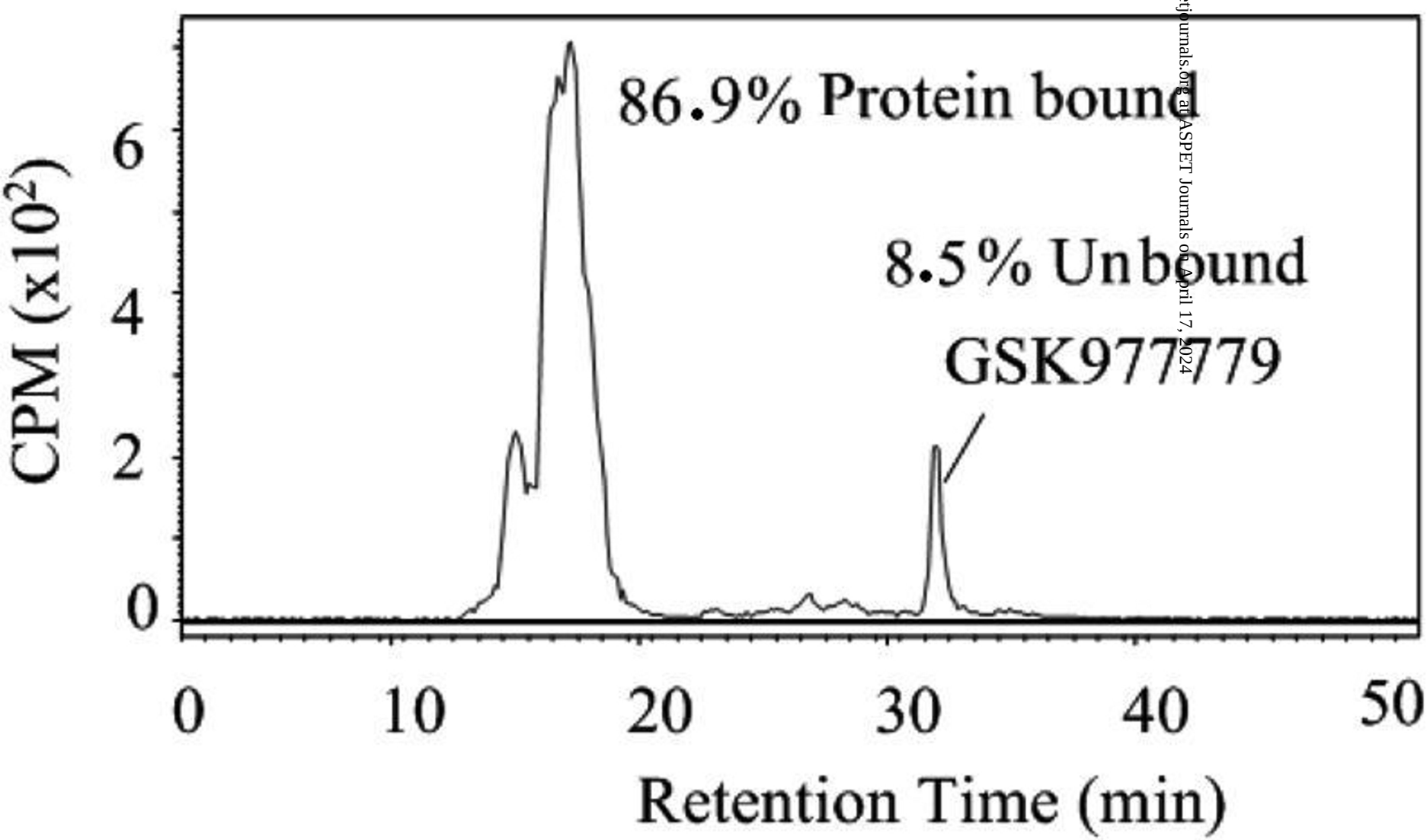

Figure 4

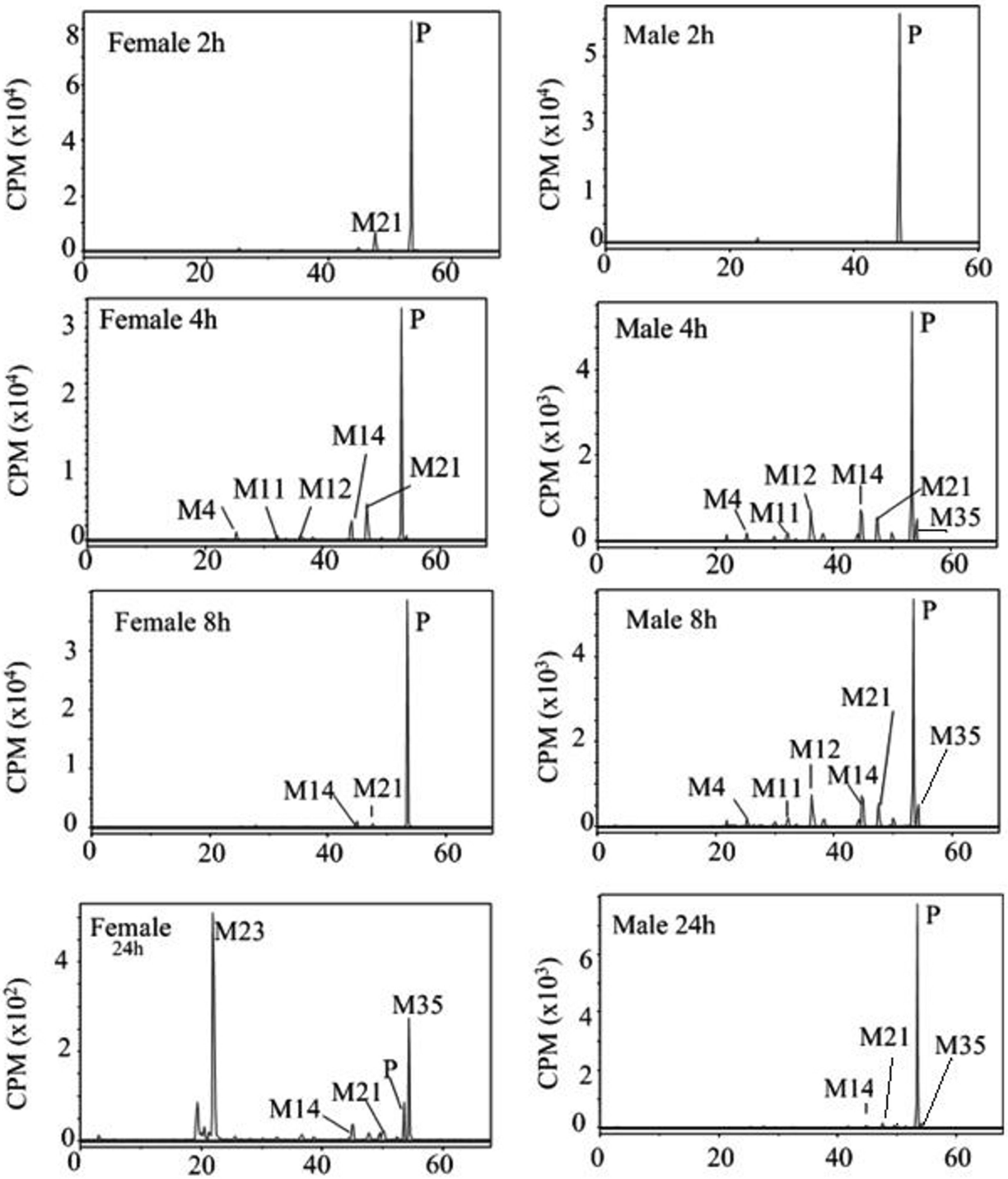

Figure 5

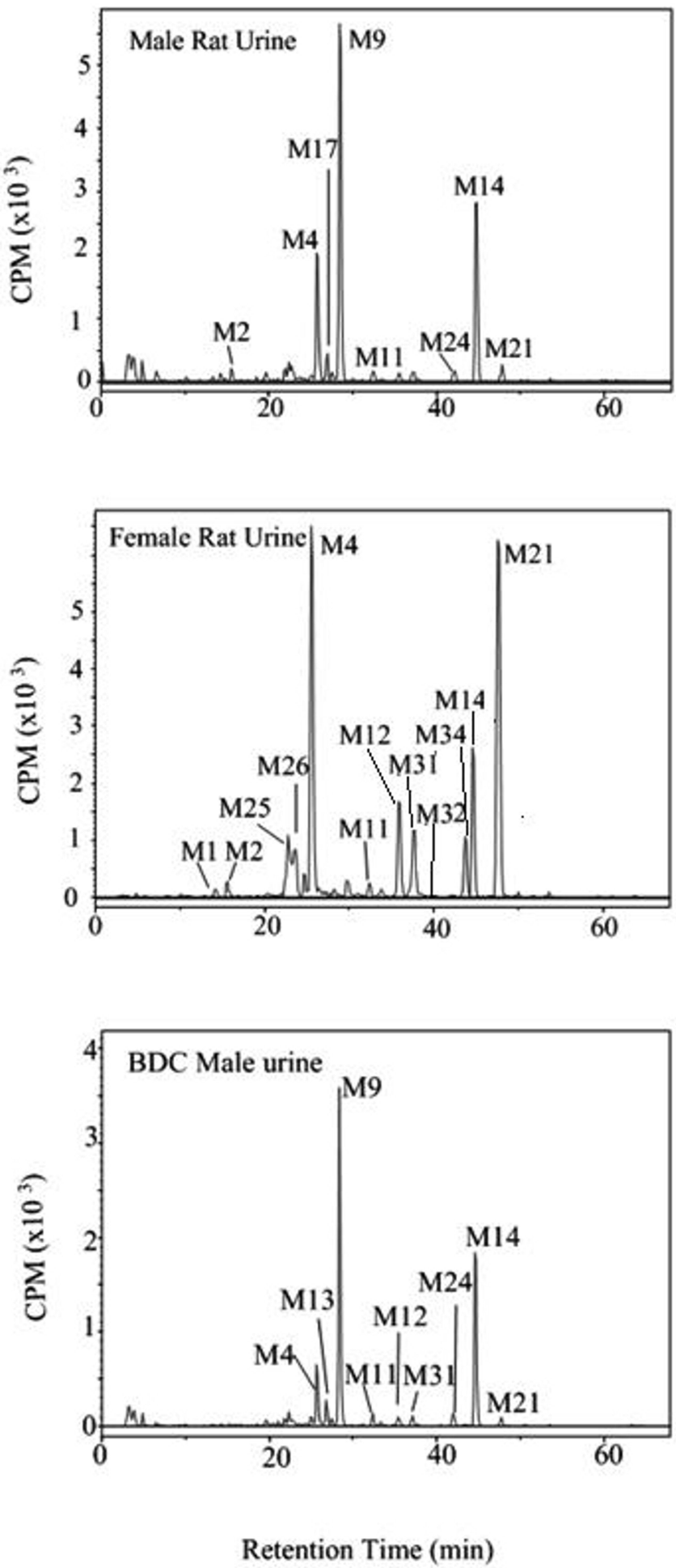

Figure 6

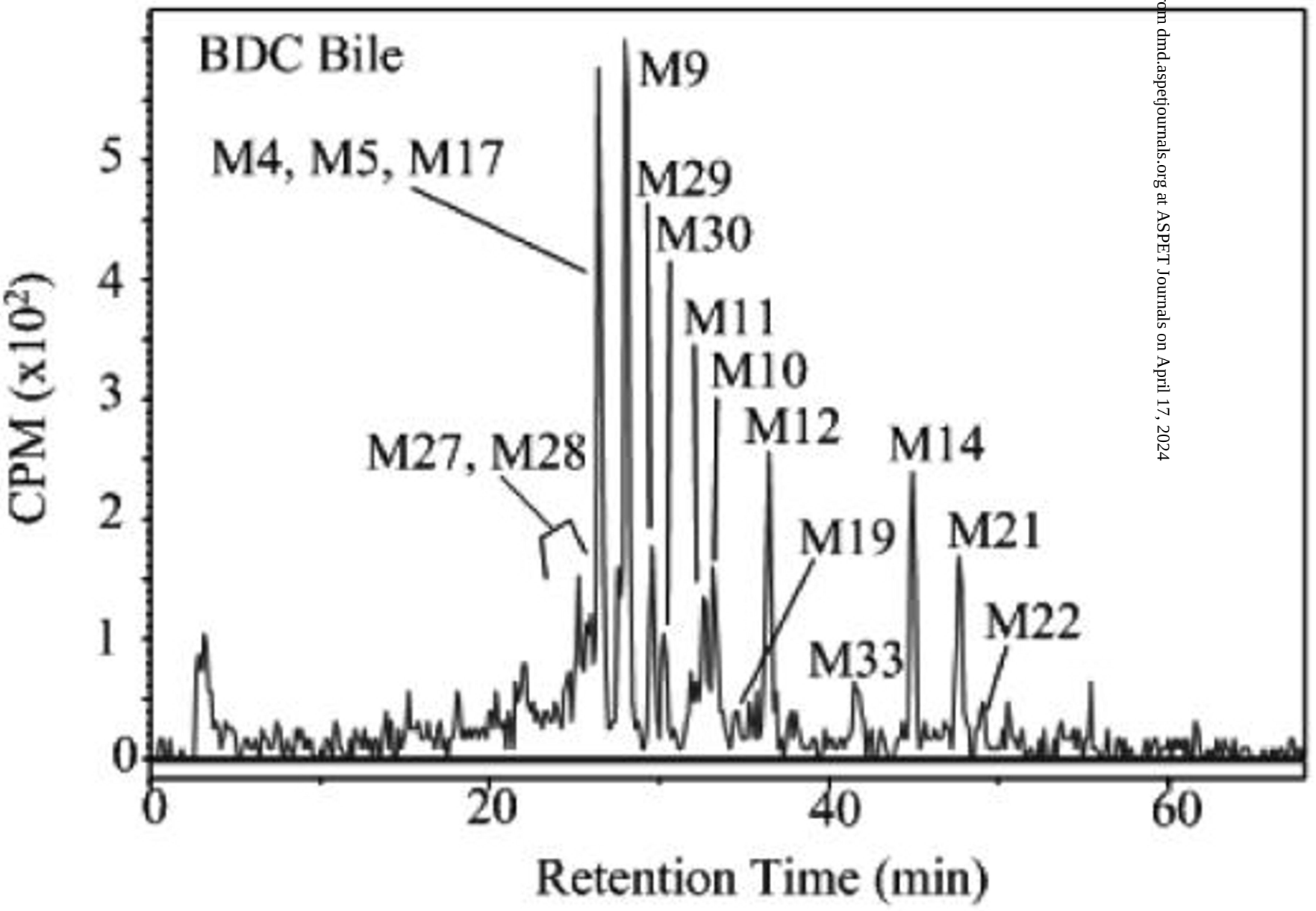

Figure 7

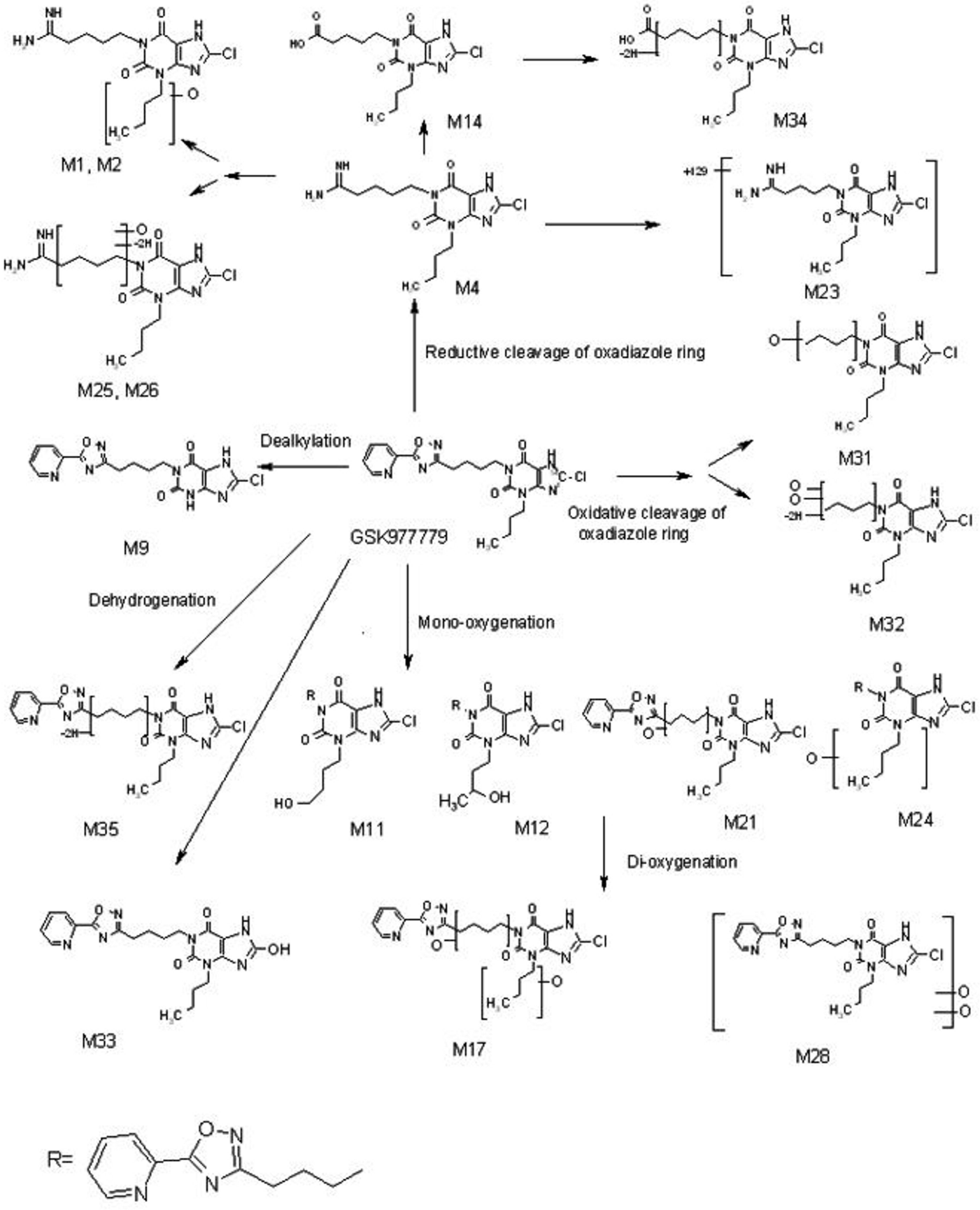

Figure 8

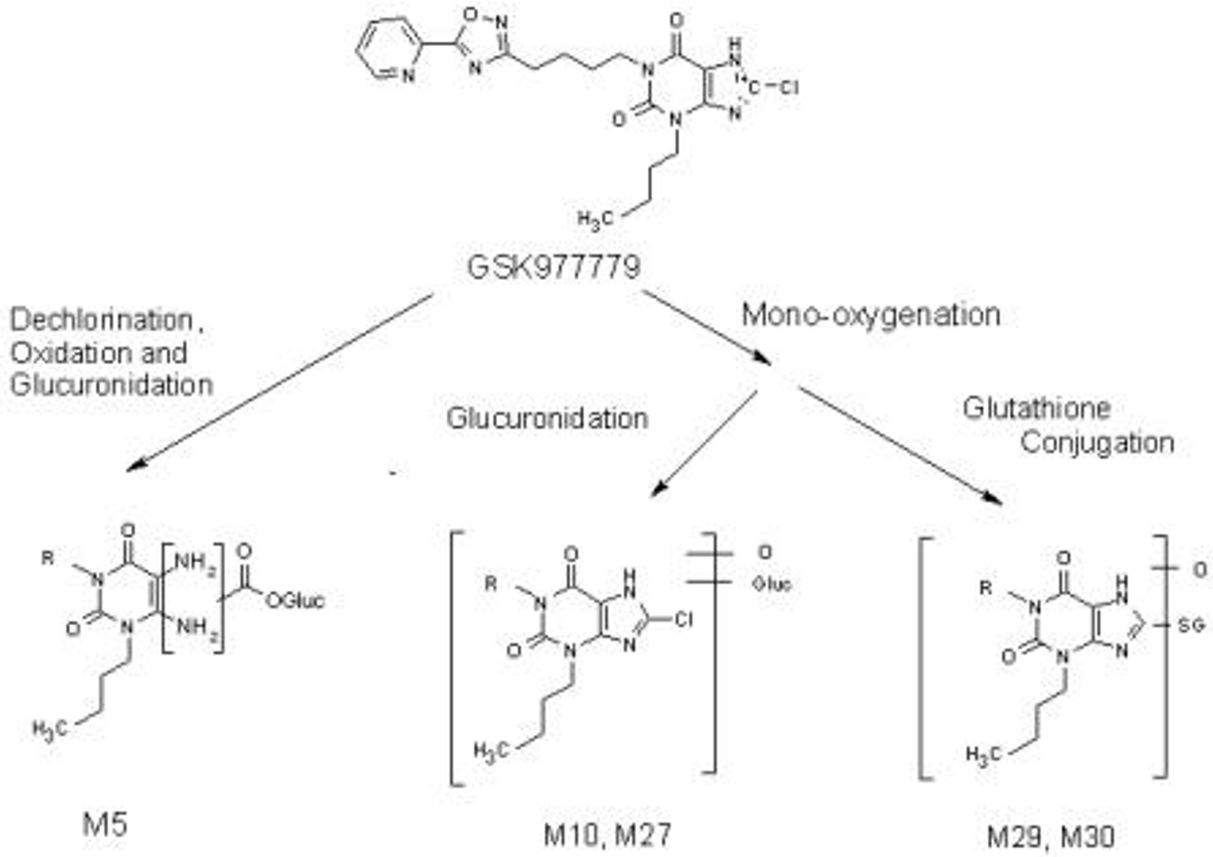

R =

GS- = Glutathione

Gluc- = Glucuronic acid

DMD Fast Forward. Published on May 31, 2011 as DOI: 10.1124/dmd.110.036467

Figure 9

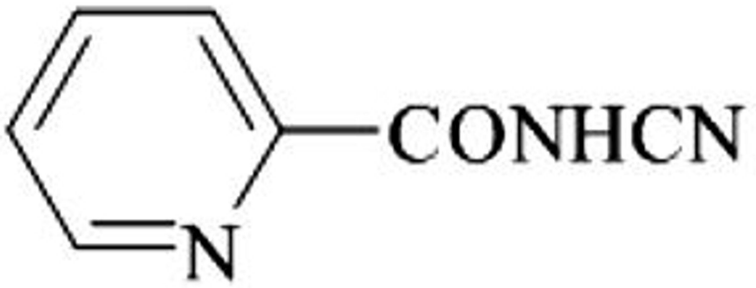

Pyridinecarboxylic acid cyanamide

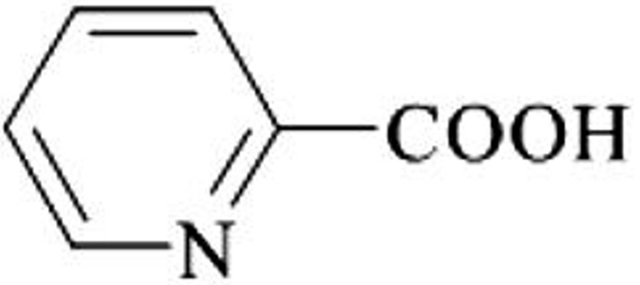

Pyridine carboxylic acid

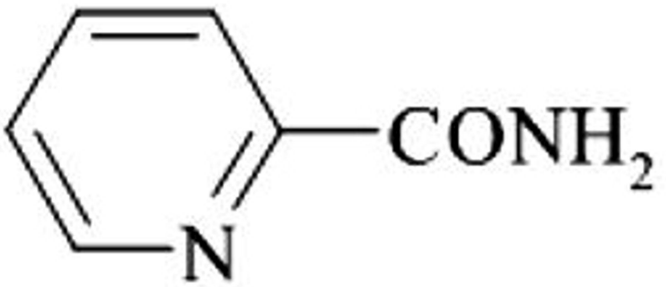

Pyridinecarboxylic acid amide

Figure 10

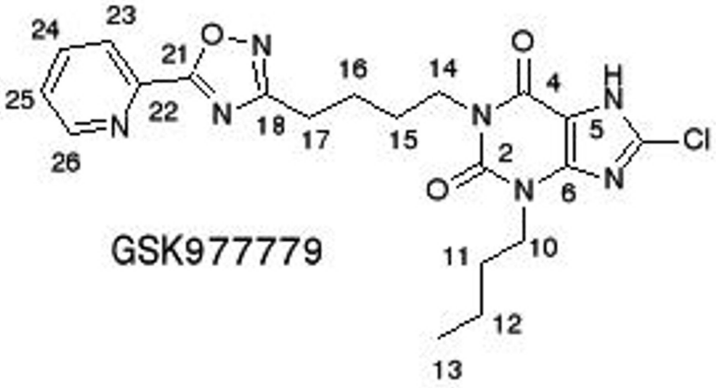

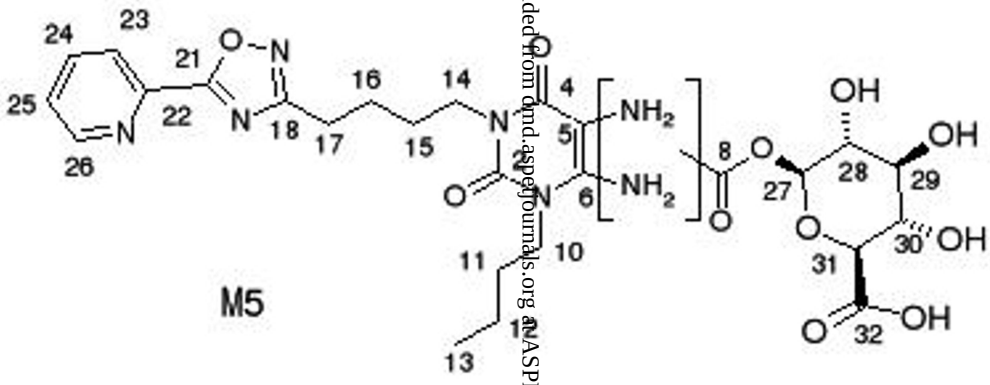

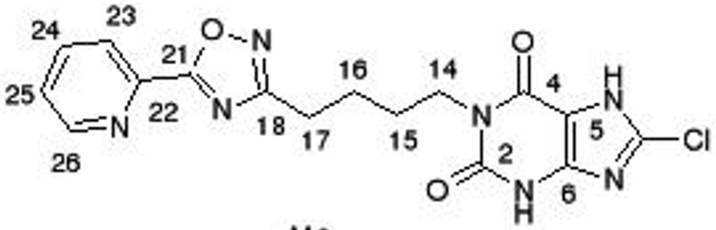

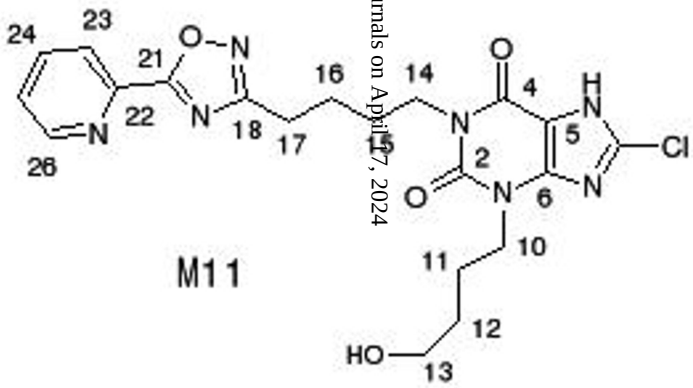

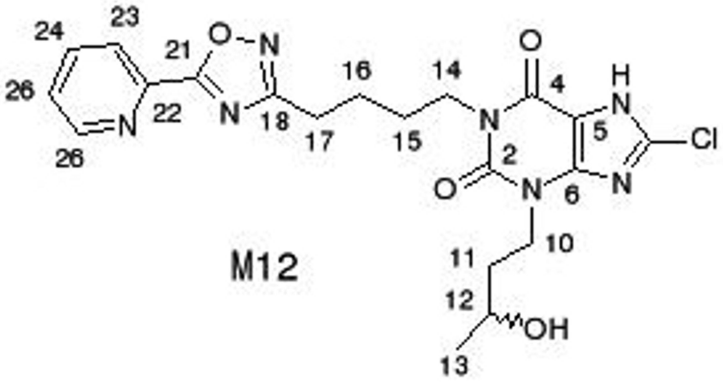

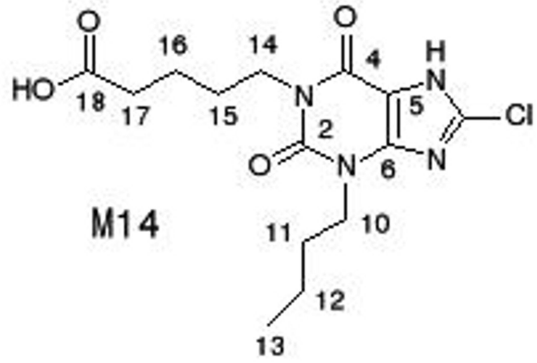

Figure 11

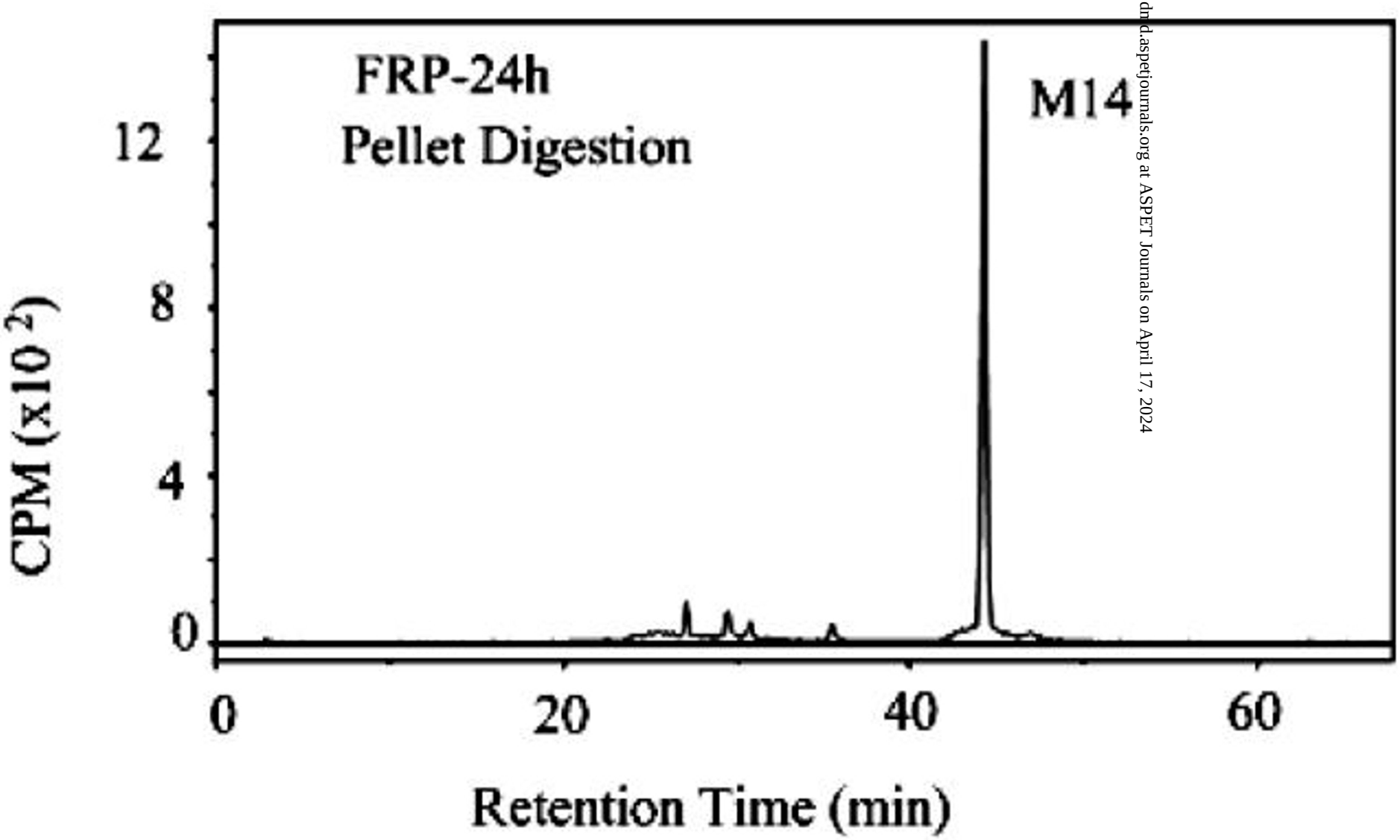

Figure 12